Dear Marc,

we uploaded the revised version of our paper.
We have made major changes to our manuscript and have addressed almost all of the reviewer's comments as described in detail below.

Many thanks for your support!

Best regards,

Thomas

---

1) Summary of the main changes

A) The motivation and description of the empirical method was improved.

We agree with both reviewers that the description of new method had errors and was complicated. It was also not well motivated.

In the revised version we shifted many technical details of the new method to the appendix (e.g. the description of our normalisation approach as new appendix A1, or the investigation of the effect of time shifts as new appendix A3).

We also added more details about the fit function to section 4, and more details about the calculation of the temporally reversed indices to section 5.1.

For the motivation of our new approach we added the following information to section 5 (see also new Fig. 6):

'... Information about the significance of the fit results can be obtained from the fit function itself. However, in practice, the significance information from the fit has several limitations:

a) The determination of the significance is based on several assumptions about the data sets, e.g. that all data points of the time series have the same uncertainties and follow a normal distribution. However, the errors of the individual data points can be very different, e.g. the effect of clouds on the errors of the satellite TCWV data set can be very different for different seasons and regions. Also, the uncertainties are not only random but contain also systematic contributions. It is difficult (if not impossible) to quantify the uncertainties of the involved time series.

b) The determination of the significance is based on prescribed significance levels. The choice of such a significance level is arbitrary and the obtained significance information depends on this choice.

c) In several tests we fitted artificial time series to the TCWV data set. These tests showed that even for such non-geophysical time series 'significant' fit results can be obtained (see the examples in Fig. 6). On the left side of this figure, fit results for a time series containing only white noise, and on the right side fit results for a temporally reversed teleconnection index are shown (the temporally reversed index is obtained from the original index by mirroring the time axis). The blue and red areas show fit coefficients for both time series, which are classified as significant by the fit.

Based on these findings, we conclude the use of the significance of the detection of an index derived from the fit itself is not straight-forward.

To address these difficulties, we developed and applied an empirical approach to determine threshold values for the delta RMS values to decide whether an index is significantly detected

in a global data set. The new procedure is described in the next section. It has the following two main advantages:

-the threshold values are determined empirically. Thus no assumptions on the properties of the time series or the significance levels have to be made.

- the method provides a clear procedure and in particular a metric which can be applied in a consistent way to different data sets and thus allows a quantitative comparison (see section 6).'

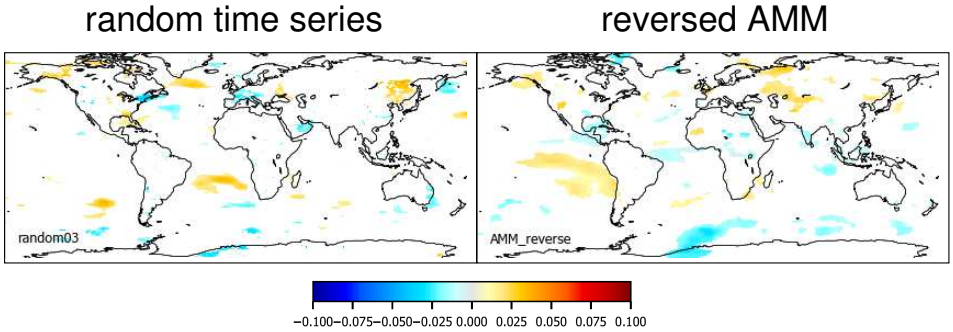

New Fig. 6 Global maps of the fit results for an artificial time series containing only white noise (left) and a temporally reversed teleconnection index (AMM, right). The white areas represent fit results, that are classified as non-significant by the fit routine (for a 5% significance level).

B) The Scope and aims were made more clear.

Probably one important misunderstanding was that we gave the impression to the reader that we aim to investigate the influence of teleconnections on the TCWV. This has probably even led to the expectation that we could predict monthly TCWV using teleconnections. This was not our intention. To make this more clear in the revised version of the manuscript, we removed the term 'influence of...', in all parts of the text. And in the introdiction we added the following information: 'Here it should be noted that we do not aim to identify causal relationships or even to predict the TCWV based on teleconnection indices' At the end of the introduction, we added more details and explanations to our research goals. We also restructured the conclusions accordingly and provided respective answers to the research questions formulated in the introduction. The following modified text was added to the conclusions:

'....Based on the obtained results, we could derive the following main conclusions related to the science questions mentioned in the introduction:

a) We developed a new empirical approach to determine whether a teleconnection index is significantly detected in a global data set. This approach avoids problems of existing algorithms for the determination of significance, because no assumptions on the significance level or the measurement uncertainties have to be made. We applied the new method to a global data set of the TCWV derived from satellite observations and found that 40 teleconnection indices could be significantly detected.

b) We applied the same method also to TCWV from the ERA interim data set. Here we used two versions of the model data sets, one including all data, the other only clear sky data. The results for both versions agree in general very well with those for the satellite data set. This confirms both the quality of the satellite and model data sets. It also indicates that the satellite observations can be seen as representative for all day mean values. For some teleconnections, however, also systematic differences, mainly over northern Africa, were obtained. Since these differences are not found for the majority of the teleconnection indices, we conclude that they are very probably not related to systematic errors of the satellite data set, but rather indicate shortcomings of the model over these regions.

c) We also applied our method to a variety of other data sets, which are usually used in teleconnection studies (surface temperature, surface pressure, geopotential heights and meridional winds at different altitudes). For most of these data sets less teleconnection indices were significantly detected than for the TCWV data sets, while for zonal winds, more teleconnection indices (up to >50) were significantly detected. These results indicate that our global TCWV data set is well suited for teleconnection studies. In our view, this is an important aspect, because our data set is exclusively based on measurements. The strongest teleconnection signals were detected for the data sets of tropospheric geopotential heights and surface pressure. This finding is consistent to the fact that most teleconnection studies are based on these quantities. Another interesting finding is that in none of the global data sets, non-teleconnection indices (like the solar variability, the stratospheric AOD or the hurricane frequency) were significantly detected.

d) We investigated the spatial distribution of the teleconnection patterns. In particular we calculated global maps for the cumulative effect of all teleconnection patterns. For that purpose we first orthogonalised the teleconnection indices to avoid the effect of correlation between the indices. Compared to the original set of indices, much less of the orthogonalised indices (20 compared to 42) were significantly detected in the TCWV data set. Our global map of the cumulative effects of all significantly detected orthogonalsed teleconnections showed the strongest teleconnection signals in the global TCWV data set over the Tropics and in polar regions. These spatial patterns point to importance of different driving mechanisms in different regions.'

C) The relationships between different indices and the motivation for the orthogonalisation of the indices was made more clear:

We added new columns in Table 2 (see below). We now show separate columns for indices similar to ENSO, polar atmospheric indices, MJO indices, as well as other oceanic and atmospheric indices.

Indices similar to ENSO (7)	**Other oceanic indices (16)**	**Atmospheric polar indices (8)**	**MJO indices (15)**	**Other atmospheric indices (8)**	**Others indices (7)**
BEST N34 TPI ONI ENSO N4 IND	HAW PDO PMM N1 TNI NTA TNA WHWP IPO CAR AMO DMI AMM STA TSA EA_ersst	SCA AAO EAWR NAO EPNP AO PE WP	MJ1 MJ2 MJN VPM1 VPM2 VPMN RMM1 RMM2 RMMN OOMI1 OOMI2 OOMIN FMO1 FMO2 FMON	PNA SOI NOI EA QBO Q30 Q50 Q70	Solar indices: RI MGII SWO S107 AP HUR (hurricane frequency) SAOD (stratospheric AOD)

In section 3 we added the following explanation:

'Many of these indices (describing the same phenomenon), but also many of the other teleconnection indices are highly correlated. The strength of these correlations is presented in Fig. 3 as a matrix with correlation coefficients between the different indices (after the seasonal cycles were removed). In spite of the correlations amongst the teleconnection indices, we decided as a first step to include them all in our study, because beforehand it is not clear which index might be best suited to represent a teleconnection phenomenon. Using our empirical approach, however, it becomes possible to quantify the significance and strength of the different indices and thus to select the best suited index for a given teleconnection phenomenon. Finally, we apply an orthogonalisation for the most significant indices (see section 7) to minimise the effect of the correlations and to identify the dominant temporal teleconnection patterns in our TCWV data set.'

To better motivate the orthogonalisation, we modified the respective information in section 7 to:

,To account for correlations between the different indices, we thus applied an orthogonalisation approach. For the orthogonalisation (based on the Gram–Schmidt process), all ,significant' original indices and significant temporal derivatives (see Figure A11) were considered (in total 57 indices). The order of indices used in the iterative orthogonalisation process was from highest to lowest p99 values. The result of the orthogonalisation approach is a set of modified teleconnection indices, which shows zero correlation amongst each other (for the considered time period). Thus this new set of orthogonalised indices can be used to determine the number of independent significant teleconnection patterns in the global water vapor data sets. We applied our new method to the new set of orthogonalised indices to test which of the modified indices have p99 values above the significance threshold.'

D) The logical flow of the paper and the appearance was improved.

As mentioned above several technical parts were shifted to the appendix. The science questions were better motivated in the introduction, and the corresponding answers were added to the conclusions.

Several Figures were shifted/deleted/modified:

-Fig. 3 was shifted to the appendix

-Fig. 8 was shifted to the appendix

-the upper part of Fig. 9 was shifted to the appendix

-Figs A1 and A2 were deleted as suggested

-the quality of Fig. A4 was improved and the number of the sub-figures was largely reduced (by a factor of 3)

-the quality of Fig. A9 was improved

E) We added a new sub-section (6.1) for the comparison of the spatial patterns of the measured and simulated TCWV.

While for most teleconnection indices very good agreement of the spatial patterns is found between the measuremed and simulated TCWV, for some indices also substantial differences are detected. These differences can point to shortcomings in either the satellite or model data sets (or both) and might be helpful for corresponding improvements.

We added a new Fig. 8 (see below) and the following new text:

'For most of the teleconnection indices, very similar spatial patterns are found in the TCWV data sets obtained from satellite or ECMWF data (see Fig. A9). This confirms both the high quality of the satellite measurements and model simulations. However, for some indices, also substantial differences are found (see Fig. 8). The most obvious differences are found over northern Africa. In principle, they could be caused by errors of both the satellite or model data sets. However, since very good agreement over northern Africa is found for most of the indices, we can very probably exclude systematic measurement biases (like e.g. effects from the high surface albedo over the Sahara). Thus we conclude that the observed differences

probably indicate deficiencies in the model simulations, possibly related to the sparseness of observational data over northern Africa used in the model. It is interesting to note that the differences are found for both oceanic and atmospheric indices which have rather different frequencies. These comparison results might help to improve the model performance over northern Africa (and to a lesser degree also over other regions).'

New Fig. 8:

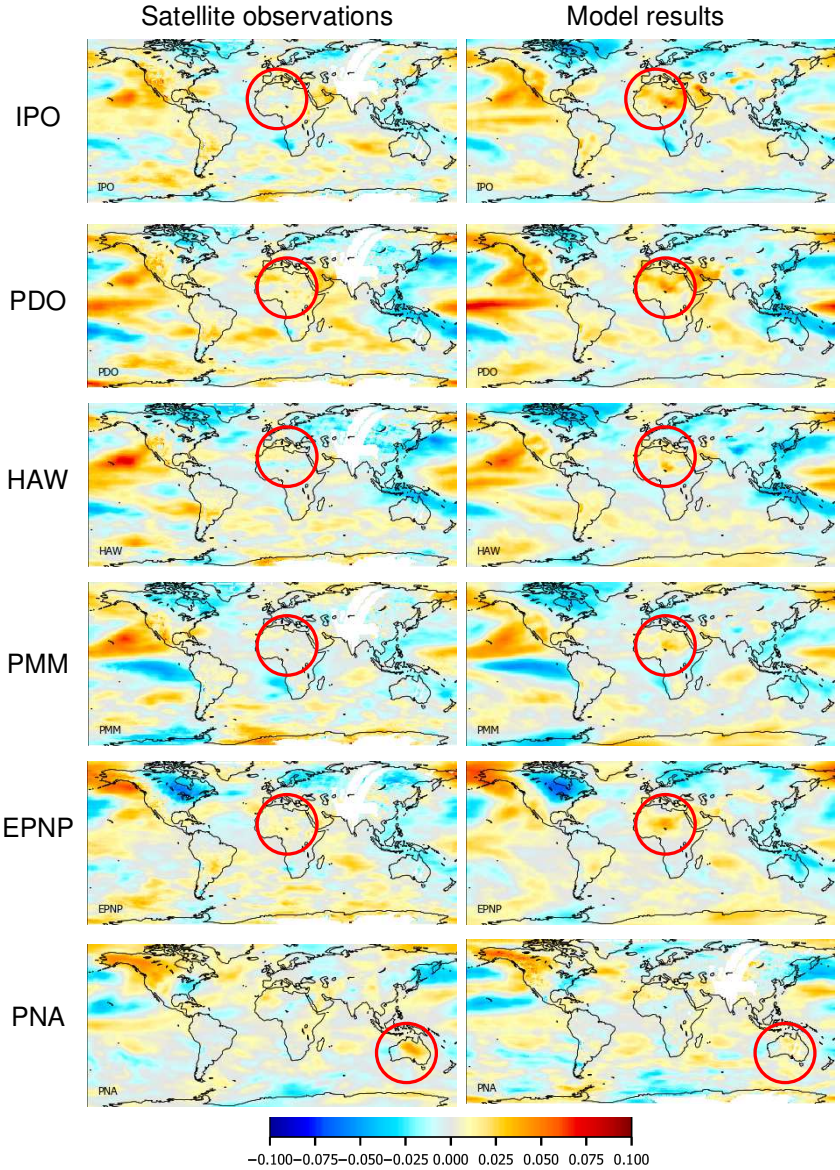

Fig. 8: Fit coefficients for selected teleconnection indices, for which different patterns were found in the TCWV data set from satellite observations (left) and model simulations (right). The red circles indicate regions with substantial differences

2) Replies to the comments of reviewer #1

Reviewer comment:
The manuscript selects extensive existing teleconnection indices and aims to identify teleconnection patterns in a new global dataset. It presents a new method to examine the reproducibility of the teleconnection in the global dataset along with other data sources. Although the manuscript first employs the dataset to the teleconnection research, which shows its novelty, the quality of the presentation needs substantial improvements. In the current version, the manuscript intends to address the research questions mentioned in the introduction, but the presentation of the results is confusing and difficult to follow. For example, the manuscript (e.g., Page 2, line 66-67) frequently mentioned the aim is to investigate the influence of teleconnections on the global distribution of the total column water vapor (TCWV). As far as I understand, the paper does not clearly address this issue. Could the authors clarify and stress the influence of teleconnection on the TCMV in the manuscript?

Author reply:
As mentioned in point B) above, we tried to make our aims more clear. Our aim was not to investigate the influence of teleconnection on the TCMV or to predict monthly TCWV using teleconnections. As described in point B) above, this was made more clear in many parts of the manuscript. For the text mentioned above (Page 2, line 66-67), we modified it to:
'In this study we investigate to which extent the temporal patterns of various teleconnections can be identified in the global distribution of the total column water vapor (TCWV).'

Reviewer comment:
Hence, I suggest some restructure of the body text of the manuscript. For instance, it might be beneficial to clarify the relationship between different groups of indices and their corresponding results.

Author reply:
We agree and made the corresponding changes, see points B), C), and D) above.

Reviewer comment:
Also, I suggest the authors improve the quality of the figures.

Author reply:
We agree and made the corresponding changes, see point D) above.

Specific comments:

Reviewer comment:
1. The manuscript used the water vapor column data from satellite observations in the red spectral range. Is there anything special for the use of red spectral range in the paper? It will be good to give some explanations otherwise I suggest removing "in the red spectral range" from the title.

Author reply:
We changed ‚red' to ‚visible'. The important point here is that the satellite observations observe scattered and reflected sun light. Thus they are sensitive for the total atmospheric column.

We added the following explanation to section 2.1:
'The data analysis is performed in the red spectral range. Since these satellite instruments observe scattered and reflected sun light, the observations are sensitive for the whole

atmospheric column including the surface-near layers which usually contain the largest fraction of the total atmospheric TCWV.'

Reviewer comment:

2. Page 3, line 105: Could the authors provide one or two references, which shows that the variations of the TCWV are strongly associated with ENSO events? Or can authors provide the correlations over the tropical band?

Author reply:

The following references were added:

Simpson, J. J., J. S. Berg, C. J. Koblinsky, G. L. Hufford, and B. Beckley, The NVAP global water vapor data set: Independent crosscomparison and multiyear variability, Remote Sens. Environ., 76, 112–129, 2001.

Soden, B. J., The sensitivity of the hydrological cycle to ENSO, J. Clim., 13, 538– 549, 2000.

Wagner, T., S. Beirle, M. Grzegorski, S. Sanghavi, U. Platt, El-Niño induced anomalies in global data sets of water vapour and cloud cover derived from GOME on ERS-2, J. Geophys. Res, 110, D15104, doi:10.1029/2005JD005972, 2005.

Reviewer comment:

3. In the third section (Page 4, line 130-145), the authors did a great piece of work on putting various existing teleconnection indices together. The manuscript divides those indices into groups but indices in the same group can have high correlations, like ENSO indices (Fig. A3). The authors could focus on some selected indices and omit other highly correlated indices unless the differences among those indices affect the conclusion of the manuscript. It would be good to see more discussions in the line 143-144 for Fig.4.

Author reply:

In this comment we see two important aspects:

a) the description of the correlations and the grouping of the indices should be improved.

We followed this suggestion, see point C) above. In particular we added new sub groups of indices to table 2.

Furthermore, we added the information that for indices with high correlation similar spatial patterns are found in the TCWV data set. In section 4.1 we added the following information:

' As expected, for groups of indices with strong temporal correlation also similar spatial patterns are found. This is most obvious for indices similar to the ENSO index (first group of indices in Figures A6 and A8). Similar spatial patterns are also found for other pairs of indices, e.g. between the Hawaiian Index (HAW) and the Pacific Decadal Oscillation (PDO) as well as between the South Tropical Atlantic index (STA) and the Equatorial Atlantic Index (EA_errst)'

b) It is suggested to ‚focus on some selected indices and omit other highly correlated indices unless the differences among those indices affect the conclusion of the manuscript.'

In principle we agree to this suggestion. However, in our opinion this was already addressed in a systematic way in the original manuscript by applying the orthogonalsiation of the teleconnection indices. Our choice to use an orthogonalsiation has the advantages that it is mathematically straight-forward and avoids any ambiguities and arbitrariness in the selection of the ‚best' index out of a group of similar indices. Overall our procedure should be seen as a two step approach: in the first step all available indices are used, because it is beforehand unclear, which of them are most significantly detected in the TCWV data set. But by applying our method to all indices, we can answer the question which indices are most significantly detected.

In a further step we then apply the orthogonalisation to obtain a new set of indices without any correlation amongst them.

To make our aims and the procedure more clear, we added the following information to the section 3:

'Many of these indices (describing the same phenomenon), but also many of the other teleconnection indices are highly correlated. The strength of these correlations is presented in Fig. 3 as a matrix with correlation coefficients between the different indices (after the seasonal cycles were removed). In spite of the correlations amongst the teleconnection indices, we decided as a first step to include them all in our study, because beforehand it is not clear which index might be best suited to represent a teleconnection phenomenon. Using our empirical approach, however, it becomes possible to quantify the significance and strength of the different indices and thus to select the best suited index for a given teleconnection phenomenon. Finally, we apply an orthogonalisation for the most significant indices (see section 7) to minimise the effect of the correlations and to identify the dominant temporal teleconnection patterns in our TCWV data set.'

In section 7 the explanation was extended to:
'To account for correlations between the different indices, we thus applied an orthogonalisation approach. For the orthogonalisation (based on the Gram–Schmidt process), all ‚significant' original indices and significant temporal derivatives (see Figure A11) were considered (in total 57 indices). The order of indices used in the iterative orthogonalisation process was from highest to lowest p99 values. The result of the orthogonalisation approach is a set of modified teleconnection indices, which shows zero correlation amongst each other (for the considered time period). Thus this new set of orthogonalised indices can be used to determine the number of independent significant teleconnection patterns in the global water vapor data sets.'

and in section 8:
'The cumulative delta RMS map for the orthogonalised indices represents the overall contribution of teleconnections to the variability of the global TCWV distribution.'

Reviewer comment:
4. In the fifth section, the manuscript uses the reversed indices but a clear explanation on the reversed indices and its meaning is needed, e.g. what is the meaning of 'reversed'. The current presentation makes Fig. 7 hard to understand.

Author reply:
The description of the reversed indices was made more clear, see point A) above. In section 5.1 the following clarification was added:
'The basic idea of our new approach is to use non-geophysical indices for the estimation of the significance level. Non-geophysical indices are indices without any temporal correlation with the temporal variations of the investigated geophysical data sets. For that purpose we chose all temporally reversed indices (see Table 2 and Fig. A6), because they cover all relevant frequencies of the true teleconnections. In practice, the time axis is flipped, that means the first entry (July 1995) will be assigned to the last month (October 2015), and so on.'

Reviewer comment:
5. Page 7, line 289-292: the results here are interesting. Could the authors provide more physical or dynamical explanations behind these results?

Author reply:
We added the following information to section 6:
'For the TCWV data sets, surface temperature and pressure, as well as most of the zonal winds, the largest p99 values are found for indices similar to ENSO. For the TCWV data sets and surface temperature, this can be expected, because the ENSO phenomenon is driven by the surface temperature (over the tropical Pacific). Accordingly, also the TCWV data sets will

be strongly affected, because the TCWV depends strongly on the temperature in the lowest atmospheric layers. The strong influence of the ENSO phenomenon (BEST index) on the zonal winds at most levels can probably be explained by the fact that large scale phenomena like ENSO can have a strong influence on the quasi-persistent zonal flow patterns in the tropics and sub-tropics. For the geopotential heights and meridional winds, the largest p99 values are found for the polar atmospheric indices (mostly AAO, but also SCA). For the geopotential heights this might be expected because the polar atmospheric indices are defined based on anomalies of the geopotential heights. Why also for the zonal winds, the largest p99 values are found for the polar atmospheric indices is, however, is not clear to us.'

We added also a comparison of the maximum p99 values to section 6 (we also added a new column to table 3). The respective text in section 6 is:
' Our new method for the determination of the significance level also allows a direct comparison of the strengths at which the different indices are detected in the different data sets. In Table 3 also the maximum p99 values of the delta RMS normalised by the corresponding significance threshold values are shown. The highest normalised p99 values are found for the geopotential heights (except the 50hPa level) and the surface pressure. This finding is consistent with the fact that these quantities are used in most teleconnection studies and many indices are even defined using these quantities. The lowest normalised p99 values are found for zonal winds, for which also the smallest numbers of significant indices are obtained. Intermediate values are found for the water vapor data sets.'

Minor comments:

Reviewer comment:
1. Page 3, line 116-117: Could the authors add more descriptions for Fig. 2?

Author reply:
The following information was added:
'Similar patterns are found in all three data sets indicating the good consistency amongst them. The highest values are found over the tropics, especially over the west Pacific. Lower values are found towards higher latitudes showing the strong dependence of the TCWV on temperature.'

Reviewer comment:
2. Page 3, line 125: I suggest removing Figs. A1 and A2.

Author reply:
Both figures were removed as suggested.

Reviewer comment:
3. Page 4, line 138: The manuscript used the word 'fit' here, but the introduction of the fit function is shown in the next section. Moving the description of the fit function here might improve the clarity. Section 3 and 4 should be organized in a logical flow.

Author reply:
We reorganised sections 3 and 4 accordingly.

Reviewer comment:
4. Page 5, line 174: Could the authors clarify the meaning of a larger or lower value of delta RMS (eq. 3)?

Author reply:
After equation 3 the following information is added:
'The delta RMS is a measure for the magnitude of the variance of a considered data set, which can be explained by the chosen teleconnection pattern. If there is high similarity of the temporal variation of an index with the temporal variation of the considered data set, the delta RMS values for both fits is large. If there is no similarity, the corresponding delta RMS value is zero.'

Also the following information is added:
'It should be noted that instead of the delta RMS values, also the correlation coefficients between the considered data set and the fit function (eq. 1) might have been used since the spatial patterns of both quantities are very similar (see Fig. A8).'

New Fig. A8:

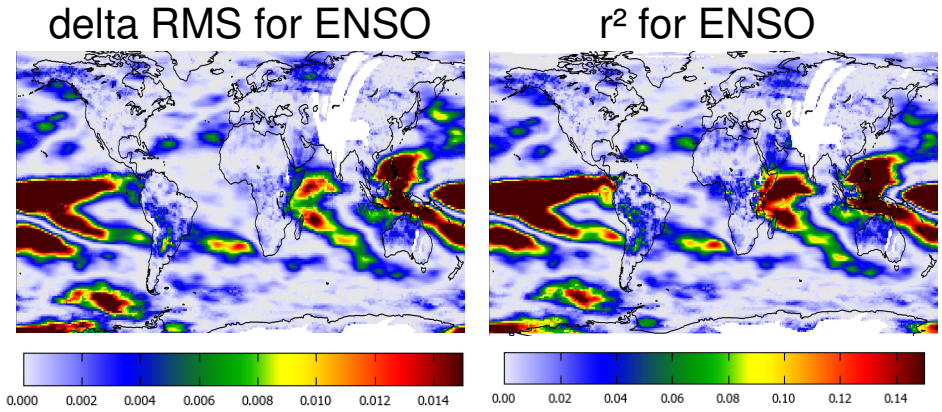

Fig. A8: Delta RMS (left) and r^2 values (right) for the fit of the ENSO index to the TCWV derived from satellite observations.

Reviewer comment:
5. Table 2 and Figure 5 captions.

Author reply:
Corrected, many thanks!

3) Replies to the comments of reviewer #2

Recommendation:
General comments: The authors are attempting to show how total column water vapor (TCWV) can be used to reveal the presence of atmospheric teleconnections seen in other datasets. This method is certainly interesting and could be of value, at least in the context of demonstrating the utility of TCWV in revealing existing teleconnections. However, the presentation in this paper was extremely difficult to follow as the authors jumped from one analysis to another with no clear direction as to why. There were many different technical approaches employed within this study, and while these likely have value in the context of what the authors' research goals are, the reasons for using the methods they employ were not well established.

Author reply:

We are thankful for this feedback and agree that our paper was partly difficult to read. We applied major restructuring and added missing information, see points B and D) above.

Reviewer comment:
Further, the authors state early in the study that they are going to compare the results with similar results from pressure, temperature, etc. fields more traditionally utilized in teleconnection studies. I did not see these comparisons.

Author reply:
It seems that here was a misunderstanding. The comparison to other data sets was one of the main aims of our study. The comparison results are shown and dicussed in section 6. We added more explanations for the findings of the comparisons to this section:
'For the TCWV data sets, surface temperature and pressure, as well as most of the zonal winds, the largest p99 values are found for indices similar to ENSO. For the TCWV data sets and surface temperature, this can be expected, because the ENSO phenomenon is driven by the surface temperature (over the tropical Pacific). Accordingly, also the TCWV data sets will be strongly affected, because the TCWV depends strongly on the temperature in the lowest atmospheric layers. The strong influence of the ENSO phenomenon (BEST index) on the zonal winds at most levels can probably be explained by the fact that large scale phenomena like ENSO can have a strong influence on the quasi-persistent zonal flow patterns in the tropics and sub-tropics. For the geopotential heights and meridional winds, the largest p99 values are found for the polar atmospheric indices (mostly AAO, but also SCA). For the geopotential heights this might be expected because the polar atmospheric indices are defined based on anomalies of the geopotential heights. Why also for the zonal winds, the largest p99 values are found for the polar atmospheric indices is, however, is not clear to us.'

We added also a comparison of the maximum p99 values to section 6 (we also added a new column to table 3). The respective text in section 6 is:
'Our new method for the determination of the significance level also allows a direct comparison of the strengths at which the different indices are detected in the different data sets. In Table 3 also the maximum p99 values of the delta RMS normalised by the corresponding significance threshold values are shown. The highest normalised p99 values are found for the geopotential heights (except the 50hPa level) and the surface pressure. This finding is consistent with the fact that these quantities are used in most teleconnection studies and many indices are even defined using these quantities. The lowest normalised p99 values are found for zonal winds, for which also the smallest numbers of significant indices are obtained. Intermediate values are found for the water vapor data sets.'

Reviewer comment:
In general, the authors focused too heavily on the significance of the relationship between their empirical estimates of the TCWV using the teleconnection index and the TCWV itself. It read more like a study attempting to predict monthly TCWV using teleconnections, not a study linking TCWV to teleconnections. Either the study should be reframed in that context or the authors need to do a better job of linking their results back to the teleconnections they are trying to predict.
Which teleconnections were predicted well? Which were predicted poorly? Why? Such discussion was absent from this study and seems directly relevant to the research objectives outlined therein.

Author reply:
We are sorry that we gave the wrong impression here. As mentioned in point B) above, our aim was not to investigate the influence of teleconnection on the TCMV or to predict monthly TCWV using teleconnections. As described in point B) above, this was made more clear in

many parts of the manuscript. In the introduction we modified the respective sentence (Page 2, line 66-67) to:
‚In this study we investigate to which extent the temporal patterns of various teleconnections can be identified in the global distribution of the total column water vapor (TCWV).'

Specific comments:

Reviewer comment:
Most of the work done in PCA-based teleconnection studies in pressure/geopotential height is confined to midlatitude and Arctic regions in the Northern Hemisphere owing to the barotropic conditions in the tropical latitudes. This should be better specified by the authors.

Author reply:
This information was added to the introduction.

Reviewer comment:
If multiple indices characterizing the same phenomena exist (e.g. MJO, ENSO), why include them all? How do you reconcile the differences in how those indices are characterizing their teleconnection and relate those differences back to your results? (Lines 135-137).

Author reply:
The same aspect was also mentioned by the other reviewer, and we tried to make our motivation and strategy more clear in the revised manuscript:
Overall our procedure should be seen as a two step approach: in the first step all available indices are used, because it is beforehand unclear, which of them are most significantly detected in the TCWV data set. But by applying our method to all indices, we can answer the question which indices are most signifcantly detected.
In a further step we then apply the orthogonalisation to obtain a new set of indices without any correlation amongst them.
To make our aims and the procedure more clear, we added the following information to the section 3:
'Many of these indices (describing the same phenomenon), but also many of the other teleconnection indices are highly correlated. The strength of these correlations is presented in Fig. 3 as a matrix with correlation coefficients between the different indices (after the seasonal cycles were removed). In spite of the correlations amongst the teleconnection indices, we decided as a first step to include them all in our study, because beforehand it is not clear which index might be best suited to represent a teleconnection phenomenon. Using our empirical approach, however, it becomes possible to quantify the significance and strength of the different indices and thus to select the best suited index for a given teleconnection phenomenon. Finally, we apply an orthogonalisation for the most significant indices (see section 7) to minimise the effect of the correlations and to identify the dominant temporal teleconnection patterns in our TCWV data set.'

In section 7 the explanation was extended to:
'To account for correlations between the different indices, we thus applied an orthogonalisation approach. For the orthogonalisation (based on the Gram–Schmidt process), all ‚significant' original indices and significant temporal derivatives (see Figure A11) were considered (in total 57 indices). The order of indices used in the iterative orthogonalisation process was from highest to lowest p99 values. The result of the orthogonalisation approach is a set of modified teleconnection indices, which shows zero correlation amongst each other (for the considered time period). Thus this new set of orthogonalised indices can be used to determine the number of independent significant teleconnection patterns in the global water vapor data sets.'

and in section 8:
‚The cumulative delta RMS map for the orthogonalised indices represents the overall contribution of teleconnections to the variability of the global TCWV distribution.'

Reviewer comment:
In the fit functions, how were the quantities *c* and *b* determined? Were they based on a fit with the satellite data, the ERA, etc.? Nothing is provided in the text in this regard.

Author reply:
We checked the explanation of the quantities used in the fit function and added some more explanation. The definition of the involved quantities should now be more clear.

Reviewer comment:
The authors discuss the use of "reversed datasets" in section 5.1. However, they provide no discussion of what was reversed. Was it just the teleconnection time series? Was it the TCWV time series? Were they reversed in time? Did you just reverse the index numbers directly, as is done frequently in pattern recognition and database type work? I don't see why, if the reverse was temporal, why the correlations didn't simply change sign but remain the same magnitude. The authors need to provide a lot more explanation on this aspect of their study as they do not really describe it in much detail. Why did you do this?

Author reply:
Obviously our explanation of the details was not sufficient here. We added more explanations here, see also point A) above.
And in section 5.1 the following clarification was added:
'...Information about the significance of the fit results can be obtained from the fit function itself. However, in practice, the significance information from the fit has several limitations:

a) The determination of the significance is based on several assumptions about the data sets, e.g. that all data points of the time series have the same uncertainties and follow a normal distribution. However, the errors of the individual data points can be very different, e.g. the effect of clouds on the errors of the satellite TCWV data set can be very different for different seasons and regions. Also, the uncertainties are not only random but contain also systematic contributions. It is difficult (if not impossible) to quantify the uncertainties of the involved time series.

b) The determination of the significance is based on prescribed significance levels. The choice of such a significance level is arbitrary and the obtained significance information depends on this choice.

c) In several tests we fitted artificial time series to the TCWV data set. These tests showed that even for such non-geophysical time series 'significant' fit results can be obtained (see the examples in Fig. 6). On the left side of this figure, fit results for a time series containing only white noise, and on the right side fit results for a temporally reversed teleconnection index are shown (the temporally reversed index is obtained from the original index by mirroring the time axis). The blue and red areas show fit coefficients for both time series, which are classified as significant by the fit.

Based on these findings, we conclude the use of the significance of the detection of an index derived from the fit itself is not straight-forward.

To address these difficulties, we developed and applied an empirical approach to determine threshold values for the delta RMS values to decide whether an index is significantly detected

in a global data set. The new procedure is described in the next section. It has the following two main advantages:

-the threshold values are determined empirically. Thus no assumptions on the properties of the time series or the significance levels have to be made.

- the method provides a clear procedure and in particular a metric which can be applied in a consistent way to different data sets and thus allows a quantitative comparison (see section 6).'

We also added information how the delta RMS values compare to the r^2 values at the end of section 5.1 (see also new Fig. A8):
'It should be noted that instead of the delta RMS values, also the correlation coefficients between the considered data set and the fit function (eq. 1) might have been used since the spatial patterns of both quantities are very similar (see Fig. A8).'

New Fig. A8:

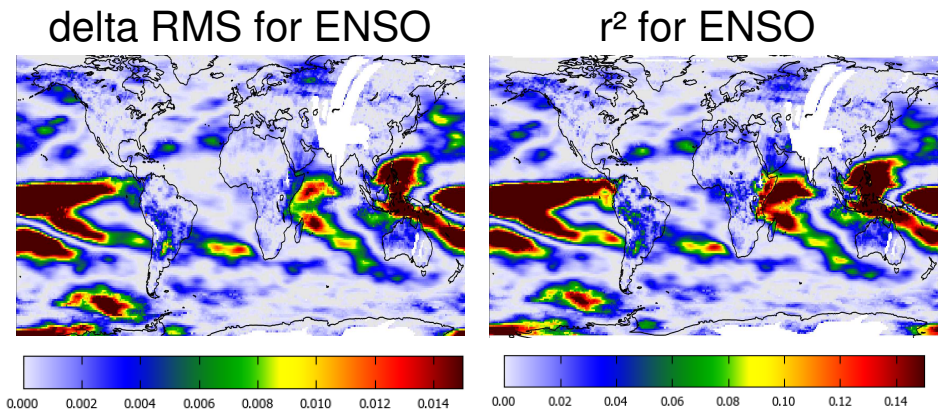

Fig. A8: Delta RMS (left) and r^2 values (right) for the fit of the ENSO index to the TCWV derived from satellite observations.

Reviewer comment:
In section 8 the authors state they "orthogonalized" their indices. What method was used to do this? Why did they do this?

Author reply:
To better explain why we applied the orthogonalisation, we modifed and extended the information given in section 7. We also added the information of the orthogonalisation technique:
'To account for correlations between the different indices, we thus applied an orthogonalisation approach. For the orthogonalisation (based on the Gram–Schmidt process), all ‚significant' original indices and significant temporal derivatives (see Figure A11) were considered (in total 57 indices). The order of indices used in the iterative orthogonalisation process was from highest to lowest p99 values. The result of the orthogonalisation approach is a set of modified teleconnection indices, which shows zero correlation amongst each other (for the considered time period). Thus this new set of orthogonalised indices can be used to determine the number of independent significant teleconnection patterns in the global water vapor data sets. We applied our new method to the new set of orthogonalised indices to test which of the modified indices have p99 values above the significance threshold.'

Technical corrections:

Reviewer comment:
The e.g. on line 51 can be removed.

Author reply:
Deleted

Reviewer comment:
What is a “time series like index”? (Line 78)

Author reply:
We replaced ‚like’ by ‚such as’ to make the meaning more clear.

Reviewer comment:
In Figures A1 and A2, are the times over which these averages were computed the same 1995-2015 time period? The ERA have a longer period of record so it would be good to specify this.

Author reply:
Both figures were deleted as suggested by the other reviewer.

Reviewer comment:
It is not clear why Figure A3 is included in the text. There are too many time series and their individual value in the study is not clear.

Author reply:
This figure was included for two reasons:
a) to add information about the sources of the different indices
b) to show the temporal patterns for the considered time period. This information is interesting for two reasons. First, the ‚frequency’ of an index can be directly recognised. Second, similarities in the temporal patterns can be easily seen.
For these reasons we decided to keep this figure in the manuscript.

Reviewer comment:
Figure A4 is almost impossible to read. There should be a compelling reason why this figure is included in the text as it includes well over 200 maps. The authors should choose which of those figures best illustrate their point and include those instead of including them all.

Author reply:
We agree that there are too many sub figures. And we want to apologise for the rather bad quality. In the revised manuscript we reduced the number of sub figures by a factor of 3 and improved the quality of the figure. We would like to keep this figure, because the global maps reveal many details of the spatial patterns found for the individual indices. It might be interesting for future studies to compare these patterns to similar results of their own analyses.

4) Revised paper with highlighted changes

Identification of atmospheric and oceanic teleconnection patterns in a 20-year global data set of the atmospheric water vapor column measured from satellites in the ~~red~~ visible spectral range

Thomas Wagner[1] and Steffen Beirle[1], Steffen Dörner[1], Christian Borger[1], Roeland Van Malderen[2]
[1]Satellite Remote Sensing Group, Max Planck Institute for Chemistry, Mainz, Germany
[2]KMI – IRM, Royal Meteorological Institute of Belgium, Brussels, Belgium

Correspondence to: Thomas Wagner (thomas.wagner@mpic.de)

Abstract. We used a global long-term (1995-2015) data set of total column water vapor (TCVW) derived from satellite observations to quantify to which extent the temporal patterns ~~the influence~~ of various teleconnections can be identified in this data set. To our knowledge, such a comprehensive global TCWV data set was rarely used for teleconnection studies. One important property of the TCWV data set is that it is purely based on observational data. We developed a new empirical method to decide whether a teleconnection index is significantly detected in the global data set. Based on this method more than 40 teleconnection indices were significantly detected in the global TCWV data set derived from satellite observations. In addition to the satellite data we also applied our method ~~also investigated the influence of teleconnection indices on~~to other global data sets derived from ERA-Interim~~ECMWF reanalysis (ERA)~~. One important finding is that the ~~results~~ spatial patterns obtained for the ERA TCWV data are very similar to the observational TCWV data set indicating a high consistency between the satellite and ERA data. Moreover, similar results are also found for two selections of ERA data (either all data or mainly clear sky data). This finding indicates that the clear-sky bias of the satellite data set is negligible for the results of this study. However, for some indices, also systematic differences in the spatial patterns between the satellite and model data set were found probably indicating possible shortcomings in the model data. For most 'traditional' teleconnection data sets (surface temperature, surface pressure, geopotential heights and meridional winds at different altitudes) a smaller number of significant teleconnection indices was found than for the TCWV data sets, while for zonal winds at different altitudes, the number of significant teleconnection indices (up to >50) was higher. The strongest teleconnection signals were found in the data sets of tropospheric geopotential heights and surface pressure. In all global data sets, no 'other indices' (solar variability, stratospheric AOD or hurricane frequency) were significantly detected. Since many teleconnection indices are strongly correlated, we also applied our method to a set of orthogonalised indices, which represent the dominant independent temporal teleconnection patterns. The number of significantly detected orthogonalised indices (20) was found to be much smaller than for the original indices (42). Based on the orthogonalised indices we derived the global spatial distribution of the cumulative ~~influence~~ effect of teleconnections ~~indices~~. The strongest ~~influence~~ effect on the TCWV is found in the tropics and high latitudes.

1 Introduction

It has been known for a long time that weather at one location can be linked to weather at a far distant location (Walker and Bliss, 1932; Bjerknes, 1966, 1969; Wallace and Gutzler, 1981; Nigam and Baxter, 2015; Feldstein and Frantzke, 2017 and references therein). The distances between such locations can be very large, up to opposite locations on the globe. The strength of the correlation varies with location exhibiting regions of maximum (anti-) correlations and regions without any significant correlation. The resulting correlation patterns are referred to as teleconnection patterns. The strongest teleconnection is the El-Nino / Southern oscillation (ENSO) phenomenon (Walker and Bliss, 1932; Bjerknes, 1966, 1969),

but many more teleconnection are known, which are located in many regions on both hemispheres (e.g. Feldstein and Frantzke, 2017 and references therein).

The temporal variability of teleconnections is usually described by teleconnection indices (e.g. the ratio of surface pressures at selected stations) and covers a wide range of frequencies from a few days to inter-annual and inter-decadal time scales (Hurrel, 1995; Feldstein, 2000; Nigam and Baxter, 2015; Woolings et al., 2015; Feldstein et al., 2017). Atmospheric teleconnections (like e.g. the North Atlantic Oscillation, NAO) have typically higher intrinsic frequencies than oceanic teleconnection indices (like e.g. the Atlantic Meridional Mode, AMM).

Teleconnections can be identified in different data sets like sea level pressure, surface air temperature, sea level pressure as well as geopotential heights and wind fields at different altitudes (Wallace and Gutzler, 1981; Thompson and Wallace, 1998; Nigam and Baxter, 2015; Feldstein and Frantzke, 2017). In recent studies, the geopotential height is the most used ~~quantity~~ variable for the quantification of teleconnections. Teleconnections are mainly found in the troposphere with the strongest amplitudes in the upper troposphere (Feldstein, 2000). But several teleconnections have also connections to the stratosphere (Feldstein, 2000 and references therein; Nigam and Baxter, 2015; Feldstein and Frantzke, 2017; Domeisen et al., 2019).

Teleconnections can be identified and defined in different ways: historically, teleconnection indices were empirically and intuitively determined based ~~e.g.~~ on the locations of meteorological stations (e.g. Walker and Bliss, 1932). In later studies more objective methods were developed based on correlation matrices, principle component analyses (PCA) (also referred to as empirical orthogonal function (EOF) methods) or rotated PCA (also referred to as varimax rotation). More details about these and further methods can be found in Horel (1981), Wallace and Gutzler (1981), Barnston and Livezey (1987), Thompson and Wallace (1998), Feldstein and Frantzke (2017) and references therein. If these methods are applied, the derived teleconnections time series and spatial patterns particularly depend on the selected region of the globe. ~~(e.g. northern hemisphere) and the selected season (e.g. winter months).~~ Most of such studies use pressure or geopotential heights and are confined to midlatitude and Arctic regions in the Northern Hemisphere because of the barotropic conditions in the tropical latitudes. ~~Usually~~Thus usually, these methods are not applied for the full globe.

Besides the fact that teleconnections are interesting in themselves, their study is also important for other applications. For example, taking teleconnections into account can improve weather forecasts (Feldstein and Frantzke, 2017 and references therein). They have impact on extreme events, e.g. heat waves, droughts, and floods (King et al., 2016; Yeh et al., 2018 and references therein) and can affect storm tracks. In addition to atmospheric quantities (e.g. humidity, precipitation, stratospheric ozone), teleconnections also affect oceanic variables (e.g. Arctic and Antarctic sea ice, the Atlantic thermohaline circulation) and the marine and terrestrial ecosystems (Feldstein and Frantzke, 2017 and references therein). Finally it is worth noting that teleconnections are expected to change in a changing climate (e.g. King et al., 2016; Feldstein and Frantzke, 2017; Yeh et al., 2018).

In this study we investigate to which extent the temporal patterns of various teleconnections can be identified in ~~the influence of various teleconnections on~~ the global distribution of the total column water vapor (TCWV). For that purpose we use a consistent long term data set (1995 – 2015) derived from satellite observations in the ~~red~~ visible spectral range obtained from GOME on ERS-2, SCIAMACHY on ENVISAT and GOME-2 on ~~METOP~~ MeTop (Beirle et al., 2018). The data sets consist~~s~~ of monthly mean values on a 1° x 1° latitude/longitude grid, which were carefully merged making use of the long overlap time between the different satellite data sets (for details see Beirle et al., 2018). Validation by independent data sets showed a smooth temporal variation with a stability within 1% over the whole period (1995-2016) (Danielczok and Schröder, 2017). To our knowledge, teleconnection studies using water vapor data sets are rare (e.g. van Malderen et al., 2018). One particular special~~i~~ty / advantage of our study is that we use for the first time a global data set which is entirely based on measurements. Here it is important to note that the TCWV is dominated by the atmospheric layers close to the surface. Another important aspect of our study is the development of a new empirical method to decide whether a teleconnection (index) can be significantly identified in an atmospheric data set or not.

Our study addresses the following main questions:

a) Which teleconnection index (and other time series ~~like~~ such as indices of solar activity) can be significantly identified in the satellite TCWV data set (or other data sets)? Here it should be noted that we do not aim to identify causal relationships or even to predict the TCWV based on teleconnection indices.

b) Are the same results obtained for TCWV data from observations and models? Here also the question is addressed how representative the satellite observations (for mainly clear sky) are for all sky data sets. Another important aspect is to compare the spatial patterns obtained for the different teleconnections between the satellite and model data sets. Such differences can give hints on possible shortcomings of the model simulations or measurements.

c) How does the number of significant teleconnections in the global TCWV data sets compare to similar results obtained for "traditional" teleconnection data sets like surface temperature, sea level pressure or wind fields and geopotential heights at different altitudes? From this comparison we can conclude whether our global TCWV data set is suited for teleconnection studies. One advantage of the use of this TCWV data set is that it is exclusively derived from measurements.

d) What is the spatial distribution of ~~the influence of~~ teleconnection patterns found in~~on~~ the global TCWV distribution? One motivation for this question is that the different teleconnections have specific drivers (e.g. tropical convection). Thus the obtained spatial distributions can give hints on the underlying mechanisms.

The paper is organised as follows: In section 2 the global data sets used in this study, and in section 3 the considered (mostly teleconnection) indices are introduced. Section 4 presents the fit function of the indices to the global data sets and the obtained global patterns. In section 5 a new method for the determination of the significance is introduced, which is applied to the different global data sets in section 6. In section 7 a reduced set of orthogonalised teleconnection indices is extracted and. Section 8 presents the global distribution of the cumulative ~~influence~~ effect of the teleconnection~~s indices~~.

2 Data sets

2.1 Total water vapor column

Our study focuses on global long term data sets of the total column water vapor (TCWV). Here we use three data sets:

a) Satellite observations from July 1995 to October 2015 (Beirle et al., 2018) derived from the satellite instruments GOME on ERS-2 (1995 to 2003), SCIAMACHY on ENVISAT (2002 to 2012) and GOME-2 on MetOp (2006 to present), which have similar overpass times (between 9:30 and 10:30 LT). The data analysis is performed in the red spectral range. Since these satellite instruments observe scattered and reflected sun light, the observations are sensitive for the whole atmospheric column including the surface-near layers which usually contain the largest fraction of the total atmospheric TCWV. The start date of the time series was predetermined by the start of the first satellite mission; the end date of the time series was set to October 2015, because some of the used time series were only available until that date. The data set is available on a 1° x 1° latitude/longitude grid with monthly resolution. The data set does not cover polar winter, since the satellite observations use scattered and reflected sun light.

In Fig. 1 the variation of the TCWV with latitude and time is shown (the latitude bins represent zonally averaged values). The top panel shows the original TCWV data set, whereas both lower panels present the absolute and relative anomalies with the mean seasonal cycle removed. Several anomaly patterns are clearly obvious, which are mainly related to strong ENSO events (see e.g. Soden, 2000; Simpson et al., 2001; Wagner et al., 2005). Especially for the relative anomalies, many high frequency variations are found. While part of these high frequency variations represent measurement noise and atmospheric noise, the results of this study showed that they also represent atmospheric teleconnections.

In addition to the satellite observations of the TCWV we also use global time series of the TCWV derived from ECMWF reanalysis (ERA Interim, Dee et al., 2011). Here we use two data sets:

a) All ERA data including clear and cloudy conditions

b) Only ERA data for clear sky observations. Here, a cloud cover below 0.3 between 1km and 6km is regarded as cloud free. This criterion reflects the observational conditions of the satellite data set.

Both data sets have a temporal resolution of 6h. For the comparison with the satellite TCWV results, ~~For both~~the ERA data ~~sets, the TCWV was~~were temporally interpolated to the time of the satellite overpass (10:00 LT). From the comparison of the results for the measurements and model data sets, the effect of the specific sampling of the satellite observations (which represent only clear sky observations) can be investigated. In Fig. 2 the global mean distributions of the TCWV data sets from satellite observations and ERA data are shown. Similar patterns are found in all three data sets indicating the good consistency amongst them. The highest values are found over the tropics, especially over the west Pacific. Lower values are found towards higher latitudes showing the strong dependence of the TCWV on temperature.

2.2 Other global data sets

Teleconnections patterns are usually derived from meteorological quantities like surface pressure and temperature or geopotential heights and wind fields at different altitudes. In this study we also consider such quantities, which we also obtained from ERA data (see Table 1). We analyse these data sets similarly to the TCWV data sets (details are described below). In this way we will assess in how far the impact of teleconnections on TCWV is comparable to traditional teleconnection data sets. ~~In Figs. A1 and A2 in the appendix, the global mean distributions of all data sets are shown.~~

3 Teleconnection indices

We performed an extensive search for teleconnection indices in the scientific literature and web sites of national weather services. We found in total 54 teleconnection indices, which cover the time span of our TCWV data set. An overview on these teleconnection indices as well as additional time series (e.g. of the solar activity) is given in Table 2. Although we do not only focus on teleconnection indices in this study, in the following we use the term 'index' to describe the whole set of teleconnection indices and other time series.

It should be noted that for several teleconnection indices (in particular for the Madden-Julian oscillation) different definitions exist. Thus the number of teleconnection indices in Table 2 is much larger than the corresponding atmospheric phenomena. Many of these indices (describing the same phenomenon), but also many of the other teleconnection indices are highly correlated. The strength of these correlations is presented in Fig. 3 as a matrix with correlation coefficients between the different indices (after the seasonal cycles were removed). In spite of the correlations amongst the teleconnection indices, we decided as a first step to include them all in our study, because beforehand it is not clear which index might be best suited to represent a teleconnection phenomenon. Using our empirical approach, however, it becomes possible to quantify the significance and strength of the different indices and thus to select the best suited index for a given teleconnection phenomenon. Finally, we apply an orthogonalisation for the most significant indices (see section 7) to minimise the effect of the correlations and to identify the dominant temporal teleconnection patterns in our TCWV data set.

A ~~more~~ detailed overview on the selected indices and their data sources is provided in Fig. ~~A3~~ A6 in the appendix.

~~Before the indices are fitted to the different global data sets, the mean seasonal cycle (1995 – 2015) is subtracted (like for the data sets themselves, see Fig. 1). Some teleconnection indices are characterised by a strong seasonal cycle, whereas others are not. In addition, also a linear trend is fitted and subtracted. Finally the obtained anomalies are normalised by the corresponding standard deviations. This ensures that the obtained fit coefficients for the different indices can be directly compared. The different steps of these preparations are illustrated in Fig. 3. It is interesting to note that many of the~~

~~considered teleconnection indices are highly correlated. Fig. 4 presents a matrix with correlation coefficients between the different indices (after the seasonal cycles were removed).~~

4 Analysis of global data sets

To determine the strength with which individual indices are detected in the temporal variations of the different global data sets, the index time series~~s~~ are fitted to the global data sets as described in section 4.1 below. Before the fit is applied, the mean seasonal cycle (1995 – 2015) and a linear trend are subtracted from the individual indices (see e.g. Horel 1981). Some teleconnection indices are characterised by strong seasonal cycles, whereas others are not. Finally the obtained anomalies are normalised by the corresponding standard deviations. This ensures that the obtained fit coefficients for the different indices can be directly compared. The different steps of these preparations are illustrated in Fig. A7. For consistency, the same steps are also applied to the different global data sets before the fit is applied.

4.1 Fit function

For each 1° x 1° latitude / longitude pixel of the global data sets (the example below is for the TCWV) the de-seasonalised time series of the monthly mean anomalies ~~of the global data sets (the example below is for the TCWV)~~ are fitted by the following function:

$$TCWV_i(t) = c + b \cdot t + f_i \cdot index_i(t) \quad (1)$$

Feldfunktion geändert

Here c and b describe constant and linear terms. $index_i$ represents the selected normalised index of monthly mean anomalies. The fit coefficient f_i describes the sign and strength of the contribution of the chosen index to the variability of the TCWV anomaly of the chosen 1° x 1° pixel. The constant offset b and possible linear trend c and the fit coefficient f_i are simultaneously determined by the fit. An example of the derived fit coefficient for the ENSO index is shown in Fig. 4 (top). Systematic patterns with positive and negative fit coefficients are found. The fit function is separately applied to the individual indices listed in Table 2. Here it should be noted that the fit function could in principle be applied to several or even all indices simultaneously. However, since many indices are highly correlated, the interpretation of the results would then not be straight forward. Thus, we chose to include the individual indices one by one in the fit function. Besides the parameters c, b, and the fit coefficient f_i, also the difference between the temporal variation of the global data sets and the applied fit function is quantified by the root mean square (RMS). The RMS for the ENSO index is shown in Fig. 4 (second row).

In order to quantify the importance of a selected index, ~~In addition to the fit function described in equation 1,~~ a second fit is performed with only the constant and linear terms:

$$TCWV(t) = c + b \cdot t \quad (2)$$

Feldfunktion geändert

The comparison of the RMS with and without including the index term (eqs. 1 and 2) allows to quantify the importance of the chosen index to describe the temporal variation of the data set. Therefore the following quantity is defined:

Formatiert: Nicht Hervorheben

$$delta\ RMS = \frac{RMS_{without\ index} - RMS_{with\ index}}{mean\ of\ data\ set(latitude)} \quad (3)$$

The RMS differences are divided by the zonal mean value (see appendix 1) of the considered quantity, because (like for water vapor) many of the analysed quantities depend strongly on latitude. The delta RMS is a measure for the magnitude of the variance of a considered data set, which can be explained by the chosen teleconnection pattern. If there is high similarity of the temporal variation of an index with the temporal variation of the considered data set, the delta RMS values for both fits is large. If there is no similarity, the corresponding delta RMS value is zero. ~~This RMS differences is then divided by the zonal mean value of the considered quantity, because (like for water vapor) many of the analysed quantities depend strongly on latitude (see equation 3). In the following this quantity is referred to as delta RMS.~~

~~$$delta\ RMS = \frac{RMS_{without\ index} - RMS_{with\ index}}{mean\ of\ data\ set(latitude)} \quad (3)$$~~

It should be noted that instead of the delta RMS values, also the correlation coefficients between the considered data set and the fit function (eq. 1) might have been used since the spatial patterns of both quantities are very similar (see Fig. A8).

The delta RMS value for the ENSO index is also shown in Fig. 4 (bottom).

The fit results i~~I~~n Fig. ~~5~~4 ~~fit results~~ for the ENSO index are ~~shown derived~~obtained for the TCWV from satellite observations (left), ERA data (center), and ERA data for clear sky conditions (right). ~~). The results for the other data sets will be discussed in section 6. The top panel in Fig. 5 shows the fit coefficients for the ENSO index.~~ High fit coefficients (Fig. 4 top) mean that a substantial part of the measured TCWV time series can be explained by the ENSO index pattern. High negative fit coefficients mean the same for the negative ENSO index. Fit coefficients of zero indicate no connection to ENSO. Very similar spatial patterns are found for the three TCWV data sets indicating that the ENSO phenomenon is well captured in the satellite and model data sets. From the similarity between the model data including all sky conditions (center) or only clear sky conditions (right) it can be concluded that the satellite observations (representing mainly clear sky conditions) are representative for all sky conditions (no obvious clear sky bias).

~~The second row in Fig. 5 presents the normalised RMS of the differences between the measurements and the fit functions. Note that in order to account for the strong latitudinal dependence of the TCWV, the RMS are normalised for each latitude bin by the mean values for all longitudes of the considered data sets.~~ In all three data sets, the smallest RMS (Fig. 4, second row) are found close to the equator. This is an interesting finding, but can probably be explained by a) the rather high TCWV and b) its rather small variability in these regions. In mid-latitudes, systematically higher RMS are found for the satellite observations compared to the model results. This is probably related to the rather large effects of clouds on the satellite observations, which becomes especially important in these regions (clouds lead to less valid observations and larger measurement uncertainties). Another interesting finding is that in polar regions the RMS for the satellite observations is smaller than for the model results. This finding is probably related to the sparseness of water vapor measurements in these regions assimilated in the ECMWF model. Thus the spatio-temporal variability of the satellite observations is probably more realistic than that of the model data. The RMS for the model results for clear sky conditions is slightly higher than for the model results for all conditions, which is to be expected because of the reduced number of data available for the cloud-filtered data set.

The lower panel of Fig. ~~5~~ 4 shows the delta RMS for the ENSO index indicating the reduction of the RMS if the ENSO index is included in the fit. As expected, the largest delta RMS is found over the tropical Pacific, where the ENSO phenomenon is most pronounced. The global distribution of the delta RMS is very similar for the three data sets. The fit coefficients and delta RMS for three other selected indices are shown in Fig. ~~6~~ 5 for the TCWV data set from satellite observations. For all indices, specific activity centers can be found in different parts of the globe. The fit coefficients ~~and delta RMS~~ for all indices are presented in the appendix (Fig. ~~A4~~A9). Note that in general very similar spatial patterns are found for the three TCWV data sets, but in some cases also systematic differences are derived (for more details see section 6.1). As expected, for groups of indices with strong temporal correlation also similar spatial patterns are found. This is most

Formatiert: Nicht Hervorheben

obvious for indices similar to the ENSO index (first group of indices in Figures A6 and A8). Similar spatial patterns are also found for other pairs of indices, e.g. between the Hawaiian Index (HAW) and the Pacific Decadal Oscillation (PDO) as well as between the South Tropical Atlantic index (STA) and the Equatorial Atlantic Index (EA errst).

~~It should be noted that in many teleconnection studies (e.g. Horel, 1981), the strength of a teleconnection index is quantified by calculating the ratio of the difference of the RMS (with and without an index included) and the total RMS. In this study we applied a different procedure as described above, because the total RMS depends on many factors, in particular also on the uncertainties of the considered data set. Since we want to compare the delta RMS values derived for different data sets (in particular the TCWV data sets derived from satellite observations and model results, but also other datasets) in a quantitative way, we decided to divide the RMS (with and without an index included) by the zonal mean of the considered data set. Thus the delta RMS shows the relative impact of the respective index. While the RMS of the different TCWV data sets are rather different (see Fig. 5, middle panel), the zonal means are very similar (Fig. 2). The zonal mean was chosen (instead of the long term average of each considered 1° x 1° pixel), because for some data sets used in this study (especially the wind data sets) large variations and even zero-crossings exist, which would lead to meaningless delta RMS values. We compared the delta RMS values calculated by our new definition with those of the more traditional definition for the TCWV data sets (Fig. A5 in the appendix). The obtained global patterns of both delta RMS definitions are almost identical.~~

~~**4.2 Quantification of the strength of a (teleconnection) index**~~

~~For a quantitative assessment of the strength and significance of a (teleconnection) index, we calculated the 99th percentile of fit indices f, for all 1° x 1° pixel values. We chose the 99th percentile because it is close to the maximum, but still not affected by individual outliers. Fig. 7 presents the 99th percentiles (p99) for all considered indices for the three TCWV data sets. For all three TCWV data sets the highest p99 values are found for the ENSO-like teleconnection indices.~~

5 Determination of significance

For most teleconnection indices spatially coherent patterns ~~clear spatial patterns~~ of fit coefficients and delta RMS values are found in the global maps (see Fig. ~~A4~~A9) indicating that these indices are significantly detected in the global water vapor data sets. These spatial patterns agree also well to the known regions where the corresponding teleconnections are active. Information about the significance of the fit results can be obtained from the fit function itself. However, in practice, the significance information from the fit has several limitations:

a) The determination of the significance is based on several assumptions about the data sets, e.g. that all data points of the time series have the same uncertainties and follow a normal distribution. However, the errors of the individual data points can be very different, e.g. the effect of clouds on the errors of the satellite TCWV data set can be very different for different seasons and regions. Also, the uncertainties are not only random but contain also systematic contributions. It is difficult (if not impossible) to quantify the uncertainties of the involved time series.

b) The determination of the significance is based on prescribed significance levels. The choice of such a significance level is arbitrary and the obtained significance information depends on this choice.

c) In several tests we fitted artificial time series to the TCWV data set. These tests showed that even for such non-geophysical time series 'significant' fit results can be obtained (see the examples in Fig. 6). On the left side of this figure, fit results for a time series containing only white noise, and on the right side fit results for a temporally reversed teleconnection index are shown (the temporally reversed index is obtained from the original index by mirroring the time axis). The blue and red areas show fit coefficients for both time series, which are classified as significant by the fit.

Based on these findings, we conclude the use of the significance of the detection of an index derived from the fit itself is not straight-forward.

To address these difficultiesHowever, from the fit results themselves it is not easily possible to judge about the significance of the detection of an index, mainly because the effects of atmospheric noise and other uncertainties of the data sets cannot easily be quantified (see also Wallace and Gutzler, 1981).

To address these difficulties, we developed and applied an empirical approach to determine threshold values for the delta RMS values to decide whether an index is significantly detected in a global data set. The new procedure is described in the next section. It has the following two main advantages:

-the threshold values are determined empirically. Thus no assumptions on the properties of the time series or the significance levels have to be made.

- p99 values. If the p99 values for a given teleconnection index is above the threshold, the index is considered as significantly detected in the considered data set. It is clear that also with this approach, for indices with p99 values close to the threshold value no clear decision about the significance can be made. The advantage of the new approach is, however, that it the method provides a clear procedure and in particular a metric which can be applied in a consistent way to different data sets and thus allows a quantitative comparison between different data sets (see section 6).

5.1 Use of reversed indices

The basic idea of our new approach is to use non-geophysical indices for the estimation of the significance level. Non-geophysical indices are indices without any temporal correlation with the temporal variations of the investigated geophysical data sets. For that purpose we chose all temporally reversed indices (see Table 2 and Fig. A6), because they cover all relevant frequencies of the true teleconnections. In practice, the time axis is flipped, Our approach for the estimation of the significance level is based on the use of reversed indices. that means the first entry (July 1995) will be assigned to the last month (October 2015), and so on. The basic idea is that the reversed indices should not contribute to the temporal variation in the global data sets, because they have no geophysical basis. Thus the derived delta RMS and p99 values can be used as an estimate of the detection limit for the significance of a fitted index for the given measurement errors of input data. In a first step, we calculate the 99th percentile of the delta RMS values of the reversed indices for all 1° x 1° pixels of the global map. We chose the 99th percentile because it is close to the maximum, but still not affected by individual outliers. The red data points in Fig. 7 presents the 99th percentiles (p99) for all reversed indices for the three TCWV data sets. From the mean value and standard deviation of the results for all temporally reversed indices, we calculate a threshold value (black dotted line in Fig. 7) for each data set (for details see appendix A2). The obtained threshold value for the TCWV data set from satellite observations is 0.0031. We also applied the same method to a set of artificial random time series and obtained a very similar threshold value of 0.0033 confirming that the threshold value obtained from the temporally reversed time series is reasonable.

If the p99 values are above the threshold, it is likely that the considered index significantly contributes to the variability of the considered data set and vice versa. For the determination of the detection limit we take into account the reversed indices of all original indices used in this study (see Table 2 and Fig. A3). This approach has the advantage that all relevant frequencies of real indices and teleconnection indices are considered.

In Fig. 7 besides the p99 values for the original temporally reversed indices (bluered), also those for the reversed original indices are shown (redblue). For many of the original indices, tThe p99 values for the reversed indices are much smaller larger than most of the original indicesthe threshold value indicating that these indices are significantly detected in the respective data set.. Interestingly, the variability of the p99 values for the reversed indices is rather high (Fig. 8). In Appendix I the reasons for this variability will be further investigated.

In addition to the use of the absolute threshold of the delta RMS values for the determination of significance, we also made use of the effect of time shifts applied to the individual indices. The underlying idea is that the delta RMS values should decrease if the original indices are de-synchronised by ± 1 month. The details of this approach are described in appendix A3. Using this additional criterion, a few more indices are added to the number of significantly detected teleconnection indices. For the TCWV data set from satellite observations, the number of significantly detected indices increases from 40 to 42, for the ERA TCWV data set from 43 to 44, and for the ERA data set for clear sky conditions from 39 to 42.

~~**5.2 Effect of shifts of the (teleconnection) indices**~~

~~In addition to the p99 values themselves, also the effect of time shifts Δt = ± 1 month of the indices on the p99 values was considered to decide whether an index was significantly identified in a global data set, because for indices with a geophysical relationship to a considered data set, the exact temporal synchronisation should be important (but might depend on region). In contrast, for indices without a geophysical relationship to the considered data set, the p99 values should not depend on the exact temporal synchronisation. In Fig. A8 the p99 values for the original and shifted (by ± 1 month) indices are shown for the TCWV data set from satellite observations. For most data sets (especially for those with high p99 values) indeed smaller p99 values are found for the shifted indices. Here it is interesting to note that in general a stronger effect is found for atmospheric indices than for oceanic indices, which can be understood by the higher frequencies of the atmospheric indices. For several oceanic indices, even higher values are found for the shifted indices indicating a time shift (mostly a time lag) between the TCWV and these indices. For one index (AMM) higher p99 values are even found for shifts in both directions indicating an ambiguity in the synchronisation between the TCWV and the AMM index.~~

~~Another interesting finding is that for some atmospheric indices with p99 values below the significance threshold (PE, MJ2, OOMI2, FMO1) still rather small ratios of the shifted and original indices are found indicating that these indices are also probably significantly detected in the TCWV data set. Thus in the following we consider also indices with p99 values below the significance threshold but with p99 ratios below 0.8 for both shifts as significantly detected. Here it should be noted that the choice of the threshold value of 0.8 is somehow arbitrary. It was chosen because a deviation of 20% from unity is larger than the 'noise level' of the ratio. The exact choice of the threshold has only a small effect on the obtained results. For the TCWV data set from satellite observations, this additional criterion increases the number of significantly detected indices from 40 to 42. For the ERA TCWV data sets the number of significantly detected indices increases from 43 to 44 (and from 39 to 42 for ERA data for clear sky conditions).~~

6 Comparison of the ~~number ‚significant indices'~~ results for the different global data sets

A rather high number of significant indices was identified in the global TCWV data sets. To put this finding into a broader perspective, we applied the same procedure also to other global data sets, which are usually considered in teleconnection studies (see Table 1). The corresponding p99 values of the different indices (including also the reversed indices) are presented in Fig. ~~A9~~A10. In general similar results as for the TCWV data sets are found. In particular, for all data sets a large number of teleconnection indices is significantly detected. However, also differences are found: in particular, the teleconnection index with the maximum p99 value is found to be different for the different data sets. For the TCWV data sets, surface temperature and pressure, as well as most of the zonal winds, the largest p99 values are found for indices similar to ENSO. For the TCWV data sets and surface temperature, this can be expected, because the ENSO phenomenon is driven by the surface temperature (over the tropical Pacific). Accordingly, also the TCWV data sets will be strongly affected, because the TCWV depends strongly on the temperature in the lowest atmospheric layers. The strong influence of the ENSO

phenomenon (BEST index) on the zonal winds at most levels can probably be explained by the fact that large scale phenomena like ENSO can have a strong influence on the quasi-persistent zonal flow patterns in the tropics and sub-tropics. For the geopotential heights and meridional winds, the largest p99 values are found for the polar atmospheric indices (mostly AAO, but also SCA). For the geopotential heights this might be expected because the polar atmospheric indices are defined based on anomalies of the geopotential heights. Why also for the zonal winds, the largest p99 values are found for the polar atmospheric indices is, however, is not clear to us.

A summary of the number of significant indices and the teleconnection index with the highest p99 is given in Table 3. Most significant indices are found for the zonal winds with the highest number in the upper troposphere. For these data sets the number of significant indices is larger than for the TCWV data sets. For geopotential heights and meridional winds, less significant indices are found (and even less than for the TCWV data sets). For geopotential heights most significant indices are found in the upper troposphere, while for the meridional winds no clear altitude dependence is observed. Also for the surface temperature and surface pressure rather low numbers (less than for the TCWV data sets) of significant indices are found. From these results we conclude that the global TCWV data sets are well suited for teleconnection studies. Here it should again be noted that the satellite TCWV data is exclusively determined from measuremensts, and the TCWV is dominated by the layers close to the surface. Thus our findings indicate that also indices which are usually detected in the middle and upper troposphere can be significantly detected in data sets which are dominated by the lower troposphere.

Our new method for the determination of the significance level also allows a direct comparison of the strengths at which the different indices are detected in the different data sets. In Table 3 also the maximum p99 values of the delta RMS normalised by the corresponding significance threshold values are shown. The highest normalised p99 values are found for the geopotential heights (except the 50hPa level) and the surface pressure. This finding is consistent with the fact that these quantities are used in most teleconnection studies and many indices are even defined using these quantities. The lowest normalised p99 values are found for zonal winds, for which also the smallest numbers of significant indices are obtained. Intermediate values are found for the water vapor data sets.

~~It is also interesting to note that for different groups of data sets specific indices with maximum p99 values were found: ENSO like indices were found for the water vapor data sets, surface temperature and for zonal winds at most altitudes (except for 950 hPa, for which AO has the highest p99 value); AAO was found for surface pressure, geopotential heights and meridional winds at 500, 200, and 50 hPa, and SCA for meridional winds at 850 and 950 hPa.~~

6.1 Comparison of the spatial patterns of the measured and simulated TCWV

For most of the teleconnection indices, very similar spatial patterns are found in the TCWV data sets obtained from satellite or ECMWF data (see Fig. A9). This confirms both the high quality of the satellite measurements and model simulations. However, for some indices, also substantial differences are found (see Fig. 8). The most obvious differences are found over northern Africa. In principle, they could be caused by errors of both the satellite or model data sets. However, since very good agreement over northern Africa is found for most of the indices, we can very probably exclude systematic measurement biases (like e.g. effects from the high surface albedo over the Sahara). Thus we conclude that the observed differences probably indicate deficiencies in the model simulations, possibly related to the sparseness of observational data over northern Africa used in the model. It is interesting to note that the differences are found for both oceanic and atmospheric indices which have rather different frequencies. These comparison results might help to improve the model performance over norther Africa (and to a lesser degree also over other regions).

7 ~~Derivatives and orthogonalised indices~~Orthogonalisation of indices

It was shown in Fig. ~~4~~ 3 that many indices are strongly correlated. Thus the numbers of ‚significant indices' obtained in the previous chapters are not useful to represent the number of independent significant indices. To account for correlations between the different indices, we thus applied an orthogonalisation approach. For the orthogonalisation (based on the Gram–Schmidt process), all ‚significant' original indices and significant temporal derivatives (see Figure A11) were considered (in total 57 indices). The order of indices used in the iterative orthogonalisation process was from highest to lowest p99 values. The result of the orthogonalisation approach is a set of modified teleconnection indices, which shows zero correlation amongst each other (for the considered time period). Thus this new set of orthogonalised indices can be used to determine the number of independent significant teleconnection patterns in the global water vapor data sets. We applied our new method to the new set of orthogonalised indices to test which of the modified indices have p99 values above the significance threshold. As expected, this number

~~This effect can be addressed by orthogonalisation of the indices before they are used for the analysis of the global data sets. Since it was found in section 5 (see Fig. A8) that for some indices time shifts led to higher p99 values, we also added the temporal derivatives of index patterns to the list of indices to be orthogonalised. The p99 values for the temporal derivatives are shown in Fig. 9 (top). In general they are much smaller than the p99 values for the corresponding original indices, but still many p99 values were found to be above the significance threshold. For the orthogonalisation, all ‚significant' original indices and temporal derivatives were considered (in total 57 indices). The orthogonalisation order was from highest p99 values to lowest p99 values. In Fig. 9 (bottom) the p99 values for the orthogonalised indices are shown. Compared to the results for the original indices, two findings are of special importance:~~

~~the number of significant indices~~ (20) ~~is~~ was found to be much smaller than for the original indices (40) confirming that many teleconnection indices are indeed highly correlated and related to the same phenomena. We also found that

~~-~~the difference between the highest p99 value (for the ONI index) and subsequent p99 values is much larger than for the original indices. This finding indicates that the temporal pattern of the ENSO phenomenon is contained in many teleconnection indices (see also Fig. 3).

The delta RMS maps for the significant orthogonalised indices (together with the delta RMS maps for corresponding original indices) are presented in Fig. ~~A10~~A12. ~~Only one temporal derivative (of ONI) was found to be significant.~~

8 Global distributions

The delta RMS maps derived for the individual indices show characteristic patterns which indicate in which regions of the globe the selected index is important or not ~~(see Fig. A4)~~. In order to assess the global distribution of the general importance of teleconnections, we added the delta RMS maps of all significant indices ~~to the figure~~. ~~Maps~~ The corresponding maps of the derived cumulative delta RMS distributions are presented in Fig. 10 for different selections of teleconnection indices and TCWV data sets. In the upper panel the patterns of all significant teleconnection indices found for the TCWV data set from satellite observations are added. In the middle panel the same is shown for the significant orthogonalised indices. The comparison again clearly indicates that many indices are highly correlated to the ENSO index. Thus, if only the orthogonalised indices are considered, the ENSO pattern, especially in the tropical Pacific, becomes relatively weaker compared to the cumulative delta RMS values in other regions. The cumulative delta RMS map for the orthogonalised indices represents the overall contribution of teleconnections to the variability of the global TCWV distribution. Our results indicate that these contributions are strong in the Tropics as well as in high latitudes. This points to potential drivers of these teleconnections, e.g. tropical convection or synoptic-scale wave breaking in jet exit regions (see e.g. Feldstein and Franzke, 2017). In the lower panel the cumulative delta RMS map for all significant orthogonalised indices for the ERA TCWV data set is shown. The derived spatial patterns are very similar to those for the satellite data set. It should, however, be noted that also for regions in high latitudes, which are not covered by the satellite observations high values are found.

Fig. 11 shows the latitudinal (top) and longitudinal (bottom) distribution of the p99 values for all significant original indices (red) and all significant orthogonalised indices (blue) detected in the TCWV data from satellite observations. As expected, the highest values (related to ENSO) are found over the equatorial east Pacific, but most indices have the strongest effects in mid and high latitudes. Interestingly, in the latitude range between –30° and +30° only for one significant orthogonalised index (besides ENSO) the maximum delta RMS is found.

9 Conclusions

We investigated ~~the influence of a~~if and how strong the temporal patterns of a large set of teleconnection indices can be identified ~~on~~ in the spatio-temporal variability of a global data set of the total column water vapor (TCWV) from 1995 – 2015 derived from satellite observations. To our knowledge, it is the first time that a global TCWV data set was used in such a detailed way in teleconnection studies (note that part of this data set was already used by van Malderen et al., 2018). Here it is important to note that the TCWV data set is purely based on observational data. Another important achievement of this study is the development of a new empirical method to decide whether a teleconnection index is significantly detected in the global data set. The method is based on temporally reversed teleconnection indices, which ensures that all relevant time scales are considered. The new method can be applied in a universal way to different data sets. In this study we applied the new method to the TCWV sets derived from satellite or model data as well to several further quantities, which are often used in teleconnection studies. Based on the obtained results, we could derive the following main conclusions related to the science questions mentioned in the introduction:

a) We developed a new empirical approach to determine whether a teleconnection index is significantly detected in a global data set. This approach avoids problems of existing algorithms for the determination of significance, because no assumptions on the significance level or the measurement uncertainties have to be made. We applied the new method to a global data set of the TCWV derived from satellite observations and found that 40 teleconnection indices could be significantly detected.

b) We applied the same method also to TCWV from the ERA interim data set. Here we used two versions of the model data sets, one including all data, the other only clear sky data. The results for both versions agree in general very well with those for the satellite data set. This confirms both the quality of the satellite and model data sets. It also indicates that the satellite observations can be seen as representative for all day mean values. For some teleconnections, however, also systematic differences, mainly over northern Africa, were obtained. Since these differences are not found for the majority of the teleconnection indices, we conclude that they are very probably not related to systematic errors of the satellite data set, but rather indicate shortcomings of the model over these regions.

c) We also applied our method to a variety of other data sets, which are usually used in teleconnection studies (surface temperature, surface pressure, geopotential heights and meridional winds at different altitudes). For most of these data sets less teleconnection indices were significantly detected than for the TCWV data sets, while for zonal winds, more teleconnection indices (up to >50) were significantly detected. These results indicate that our global TCWV data set is well suited for teleconnection studies. In our view, this is an important aspect, because our data set is exclusively based on measurements. The strongest teleconnection signals were detected for the data sets of tropospheric geopotential heights and surface pressure. This finding is consistent to the fact that most teleconnection studies are based on these quantities. Another interesting finding is that in none of the global data sets, non-teleconnection indices (like the solar variability, the stratospheric AOD or the hurricane frequency) were significantly detected.

d) We investigated the spatial distribution of the teleconnection patterns. In particular we calculated global maps for the cumulative effect of all teleconnection patterns. For that purpose we first orthogonalised the teleconnection indices to avoid the effect of correlation between the indices. Compared to the original set of indices, much less of the orthogonalised indices (20 compared to 42) were significantly detected in the TCWV data set. Our global map of the cumulative effects of all

significantly detected orthogonalsed teleconnections showed the strongest teleconnection signals in the global TCWV data set over the Tropics and in polar regions. These spatial patterns point to importance of different driving mechanisms in different regions.

~~Based on this method more than 40 teleconnection indices were significantly detected in the global TCWV data set derived from satellite observations. Very similar results were obtained for two TCWV data sets from the ECMWF reanalysis (one data set uses all data, the other only clear sky data points). From these findings we conclude 1) that the spatio-temporal variability is well captured by both the satellite observations and the ERA Interim data, and 2) that a possible clear sky bias is negligible.~~

~~We also applied the method to other data sets derived from the ECMWF reanalysis and compared the results to those for the TCWV data sets. For most 'traditional' teleconnection data sets (surface temperature, surface pressure, geopotential heights and meridional winds at different altitudes) less teleconnection indices were significantly detected than for the TCWV data sets, while for zonal winds at different altitudes, more significant teleconnection indices (up to >50) were significantly detected. For most data sets the strongest teleconnection signals were found for ENSO or AAO. For some data sets the strongest teleconnection signals were found for SCA and AO. It should be noted that in none of the global data sets, other indices (like the solar variability, the stratospheric AOD or the hurricane frequency) were significantly detected.~~

~~Since many teleconnection indices are strongly correlated, we also applied our method to the orthogonalised indices. Compared to the original indices, much less orthogonalised indices (20 compared to 42) were significantly detected in the TCWV data set from satellite observations. We investigated the spatial patterns of these orthogonalised indices and found the strongest influence on the TCWV in the tropics and high latitudes.~~

Acknowledgements

We want to thank the European Centre for Medium-Range Weather Forecasts (ECMWF) and many scientific and national institutions for making meteorological data and teleconnection indices available. We also thank ESA and EUMETSAT for making satellite spectra available. We are grateful to Holger Sihler for his valuable feedback and suggestions about the discussion of the significance derived from the fit.

Data availability

The TCWV data from satellite observations are available through Beirle et al. (2018). Other data sets are available from the authors on request.

Author contributions

Thomas Wagner initiated this study. Thomas Wagner and Steffen Beirle performed the data analysis. Steffen Dörner extracted the ECMWF data sets. Thomas Wagner, Steffen Beirle, Steffen Dörner, Christian Borger and Roeland Van Malderen contributed to the interpretation of the results of this study.

Competing interests

There are no competing interests.

Formatiert

Formatiert: Englisch (USA)

Formatiert

Formatiert: Englisch (USA)

Formatiert

Formatiert: Englisch (USA)

References

Barnston, A.G., Livezey, R.E., Classification, seasonality and persistence of low frequency atmospheric circulation patterns. Monthly Weather Review 115, 1083–1126, 1987.

Beirle, S., Lampel, J., Wang, Y., Mies, K., Dörner, S., Grossi, M., Loyola, D., Dehn, A., Danielczok, A., Schröder, M., and Wagner, T.: The ESA GOME-Evolution "Climate" water vapor product: a homogenized time series of H_2O columns from GOME, SCIAMACHY, and GOME-2, Earth Syst. Sci. Data, 10, 449-468, https://doi.org/10.5194/essd-10-449-2018, 2018.

Bjerknes, J., A possible response of the atmospheric Hadley circulation to equatorial anomalies of ocean temperature. Tellus, 18, 820–829, 1966.

Bjerknes, J., Atmospheric teleconnections from the equatorial Pacific. Monthly Weather Review, 97, 163–172, 1969.

Dee, D. P., S. M. Uppala A. J. Simmons P. Berrisford P. Poli S. Kobayashi U. Andrae M. A. Balmaseda G. Balsamo P. Bauer P. Bechtold A. C. M. Beljaars L. van de Berg J. Bidlot N. Bormann C. Delsol R. Dragani M. Fuentes A. J. Geer L. Haimberger S. B. Healy H. Hersbach E. V. Hólm L. Isaksen P. Kållberg M. Köhler M. Matricardi A. P. McNally B. M. Monge-Sanz J.-J. Morcrette B.-K. Park C. Peubey P. de Rosnay C. Tavolato J.-N. Thépaut F. Vitart, The ERA-Interim reanalysis: configuration and performance of the data assimilation system, Q. J. R. Meteorol. Soc. 137: 553–597, 2011.

Danielczok, A. and Schröder, M.: GOME Evolution "Climate" product validation report, available at: https://earth.esa.int/documents/700255/1525725/GOME_EVL_L3_ValRep_final/db7e72c3-044d-4236-9dee-d88405b89ef0, 2017.

Domeisen, D.I.V., C.I. Garfinkel, and A.H. Butler, The Teleconnection of El Niño Southern Oscillation to the Stratosphere, Reviews of Geophysics, 57, 5–47, 2019.

Feldstein, S. B., Teleconnections and ENSO: The timescale, power spectra, and climate noise properties. Journal of Climate, 13, 4430–4440, 2000.

Feldstein, S. B., and C. L. E. Frankze, Atmospheric Teleconnection Patterns, in ‚Nonlinear and Stochastic Climate Dynamics', C. L. E. Franzke and T. J. O'Kane, Eds., Cambridge University Press, 54-104, 2017.

Horel, J. D., A rotated principal component analysis of the interannual variability of the Northern Hemisphere 500 mb height field. Monthly Weather Review, 109, 2080 - 2092, 1981.

Hurrell, J. W., Decadal trends in the North Atlantic Oscillation: regional temperatures and precipitation. Science, 269, 676–679, 1995.

Khaykin, S. M., Godin-Beekmann, S., Keckhut, P., Hauchecorne, A., Jumelet, J., Vernier, J.-P., Bourassa, A., Degenstein, D. A., Rieger, L. A., Bingen, C., Vanhellemont, F., Robert, C., DeLand, M., and Bhartia, P. K.: Variability and evolution of the midlatitude stratospheric aerosol budget from 22 years of ground-based lidar and satellite observations, Atmos. Chem. Phys., 17, 1829–1845, https://doi.org/10.5194/acp-17-1829-2017, 2017.

King, A. D., van Oldenborgh, G. J., & Karoly, D. J., Climate change and El Nino increase likelihood of Indonesian heat and drought, Bulletin of the American Meteorological Society, 97, S113–S117, 2016.

Nigam, S., & Baxter, S., General Circulation of the Atmosphere: Teleconnections. Encyclopedia of Atmospheric Sciences, 3, 90–109, 2015.

Simpson, J. J., J. S. Berg, C. J. Koblinsky, G. L. Hufford, and B. Beckley, The NVAP global water vapor data set: Independent crosscomparison and multiyear variability, Remote Sens. Environ., 76, 112–129, 2001.

Soden, B. J., The sensitivity of the hydrological cycle to ENSO, J. Clim., 13, 538– 549, 2000.

Thompson, D. W. J., and J. M. Wallace, The Arctic Oscillation signature in the wintertime geopotential height temperature fields. Geophysical Research Letters, 25, 1297–1300, 1998.

Van Malderen, R., Pottiaux, E., Stankunavicius, G., Beirle, S., Wagner, T., Brenot, H., and Bruyninx, C.: Interpreting the time variability of world-wide GPS and GOME/SCIAMACHY integrated water vapour retrievals, using reanalyses as auxiliary tools, Atmos. Chem. Phys. Discuss., https://doi.org/10.5194/acp-2018-1170, 2018.

Wagner, T., S. Beirle, M. Grzegorski, S. Sanghavi, U. Platt, El-Niño induced anomalies in global data sets of water vapour and cloud cover derived from GOME on ERS-2, J. Geophys. Res, 110, D15104, doi:10.1029/2005JD005972, 2005.

Walker, G. T., and E.W. Bliss, World weather V. Mem. Royal Meteorological Society, 4, 53–84, 1932.

Wallace, J.M., Gutzler, D.S., Teleconnections in the geopotential height field during the northern hemisphere winter. Monthly Weather Review 109, 784–812, 1981.

Wheeler, M. C. and H. H. Hendon, An all-season real-time multivariate MJO index: Development of an index for monitoring and prediction. *Mon. Wea. Rev.*, **132**, 1917-1932, 2004.

Woolings, T., C. Franzke, D. Hodson, B. Dong, E. Barnes, C. Raible and J. Pinto,
Contrasting interannual and multidecadal NAO variability. Climate Dynamics, 45,
539–556, 2015.

Yeh, S.-W., Cai, W., Min, S.-K., McPhaden, M. J., Dommenget, D., Dewitte, Matthew Collins , Karumuri Ashok, Soon-Il An, Bo-Young Yim, B., Kug, J.-S., ENSO atmospheric teleconnections and their response to greenhouse gas forcing. Reviews of Geophysics, 56, 185–206, 2018.

Tables

Table 1: Meteorological data sets used in this study

Quantity	Source	Altitude
Water vapor VCD	Satellite observations	Total colum
Water vapor VCD	ECMWF reanalysis (all sky conditions)	Total colum
Water vapor VCD	ECMWF reanalysis (clear sky conditions)	Total colum
Surface temperature	ECMWF reanalysis (all sky conditions)	Surface
Surface pressure	ECMWF reanalysis (all sky conditions)	Surface pressure extrapolated to sea level
Geopotential heights	ECMWF reanalysis (all sky conditions)	50hPa, 200hPa, 500hPa, 850hPa, 950hPa
Zonal winds	ECMWF reanalysis (all sky conditions)	50hPa, 200hPa, 500hPa, 850hPa, 950hPa
Meridional winds	ECMWF reanalysis (all sky conditions)	50hPa, 200hPa, 500hPa, 850hPa, 950hPa

*the zonal winds at 50hPa are not further analysed, because they are – by definition - dominated by the QBO teleconnection signal.

Table 2: Teleconnection indices and other time series used in this study~~.~~. More details about these indices as well as their sources are given in Fig. ~~A3~~ A6 in the appendix.

Indices similar to ENSO (7)	Other oceanic indices (16)	Atmospheric polar indices (~~7~~8)	MJO indices (~~7~~15)	Other atmospheric indices (8)	Others indices (7)
BEST	HAW	SCA	MJ1	PNA	Solar indices:
N34	PDO	AAO	MJ2	SOI	RI
TPI	PMM	EAWR	MJN	NOI	MGII
ONI	N1	NAO	VPM1	EA	SWO
ENSO	TNI	EPNP	VPM2	QBO	S107
N4	NTA	AO	VPMN	Q30	AP
IND	TNA	PE	RMM1	Q50	
	WHWP	WP	RMM2	Q70	HUR (hurricane frequency)
	IPO		RMMN		
	CAR		OOMI1		SAOD (stratospheric AOD)
	AMO		OOMI2		
	DMI		OOMIN		
	AMM		FMO1		
	STA		FMO2		
	TSA		FMON		
	EA_ersst				

Formatiert

Formatiert

Table 3: Numbers of significant indices and most significant indices for all data sets (the number of indices with p99 values below threshold but shift ratios <0.8 are indicated in brackets). The complete list of significant indices for the different data sets is provided in Table A1 in the appendix.

Data set	Number of significant indices	Most significant index	Maximum relative significance p99 delta RMS value
TCWV sat	42 (2)	ONI	9.9
TCWV ERA	44 (1)	ONI	12.6
TCWV ERA clear	42 (3)	ONI	11.6
Tsurf (surface temperature)	37 (1)	ONI	6.6
Spred (surface pressure)	35 (1)	AAO	19.1
Geopot 50 hPa	17 (5)	AAO	8.7
Geopot 200 hPa	40 (0)	AAO	23.3
Geopot 500 hPa	32 (1)	AAO	21.4
Geopot 850 hPa	33 (1)	AAO	20.2
Geopot 950 hPa	30 (1)	AAO	19.0
Zonal winds 200 hPa	51 (0)	BEST	15.0
Zonal winds 500 hPa	49 (0)	BEST	7.2
Zonal winds 850 hPa	46 (1)	BEST	11.0
Zonal winds 950 hPa	42 (4)	AO	11.8
Meridional winds 50 hPa	24 (3)	AAO	2.9
Meridional winds 200 hPa	32 (1)	AAO	5.4
Meridional winds 500 hPa	34 (0)	AAO	4.5
Meridional winds 850 hPa	33 (0)	SCA	6.1
Meridional winds 950 hPa	32 (0)	SCA	6.0

Figures

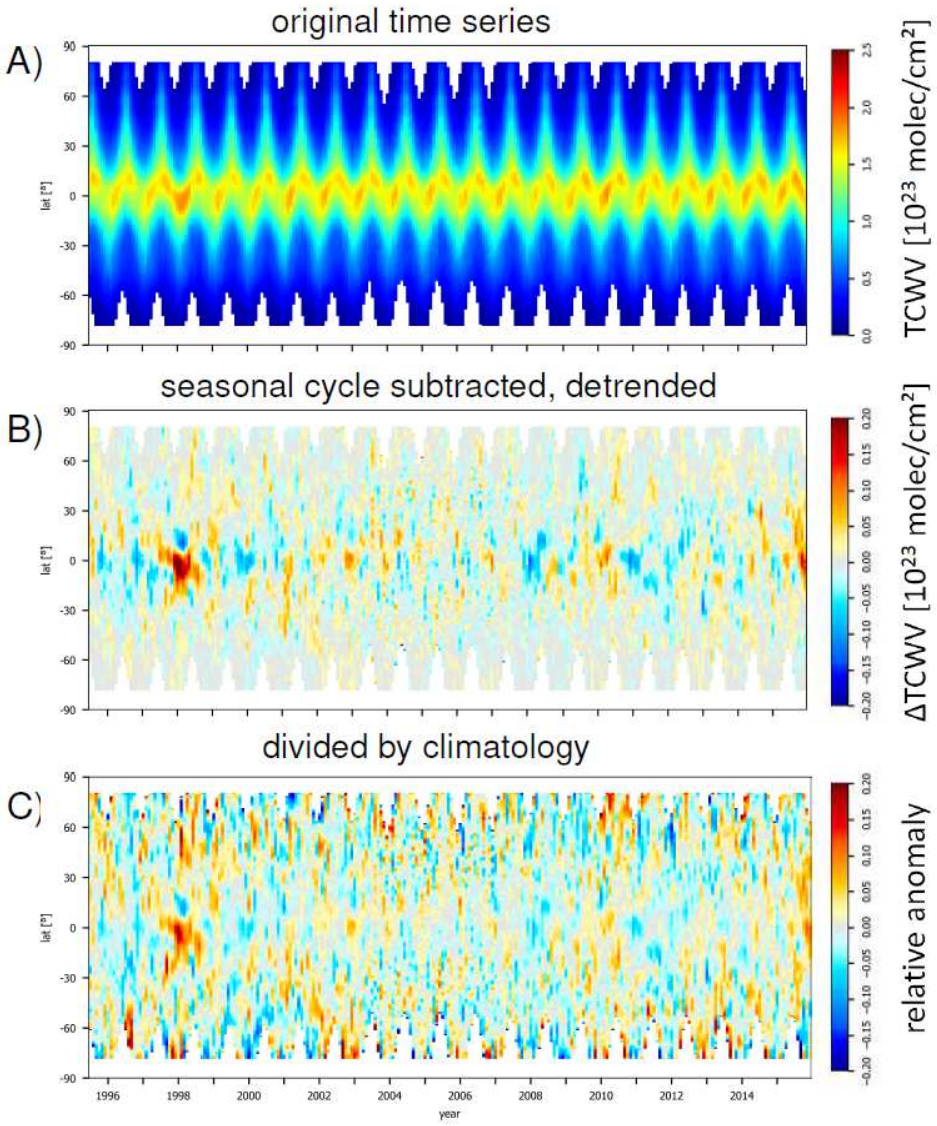

Fig. 1: A) TCWV measured from satellite as a function of time and latitude (zonally averaged values) on a 1° x 1° latitude/longitude grid with monthly resolution. B) (absolute anomalies) after the mean seasonal cycle and a linear trend was subtracted. C) relative anomalies (absolute anomalies divided by the corresponding monthly mean TCWV).

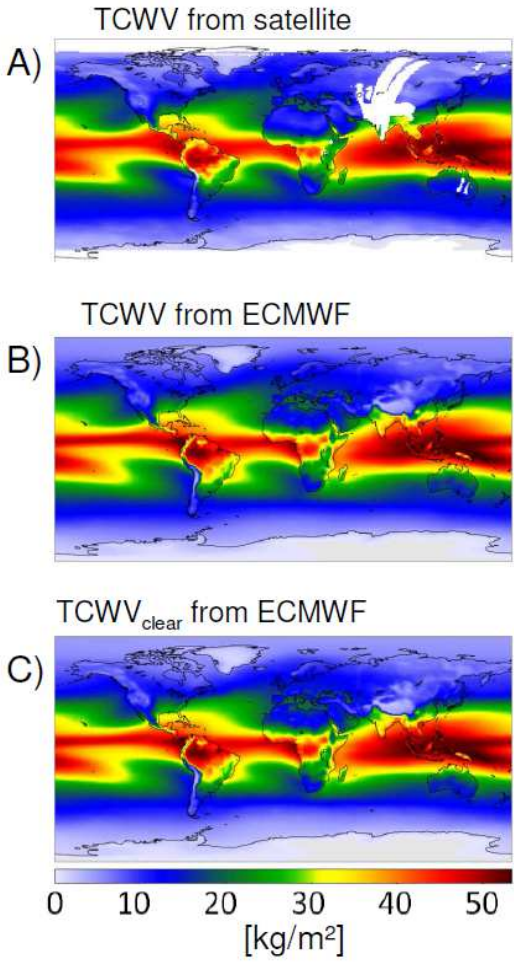

Fig. 2: Global mean distribution of the TCWV from satellite observations (A) and ERA data: B) all data; C) only clear sky observations during day.

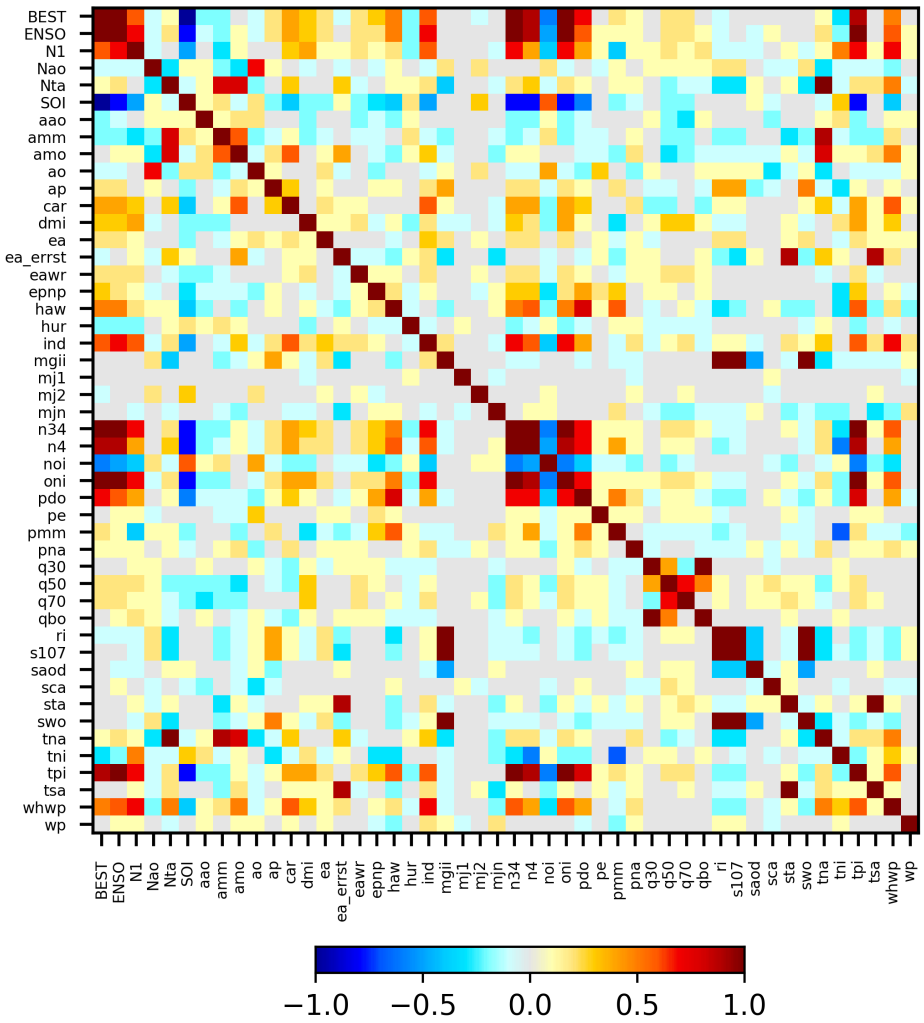

Fig. 43: Correlation coefficients between the different teleconnection indices (after seasonal cycle was removed). Note that only one set of MJO indices is included here to minimise the total number of indices.

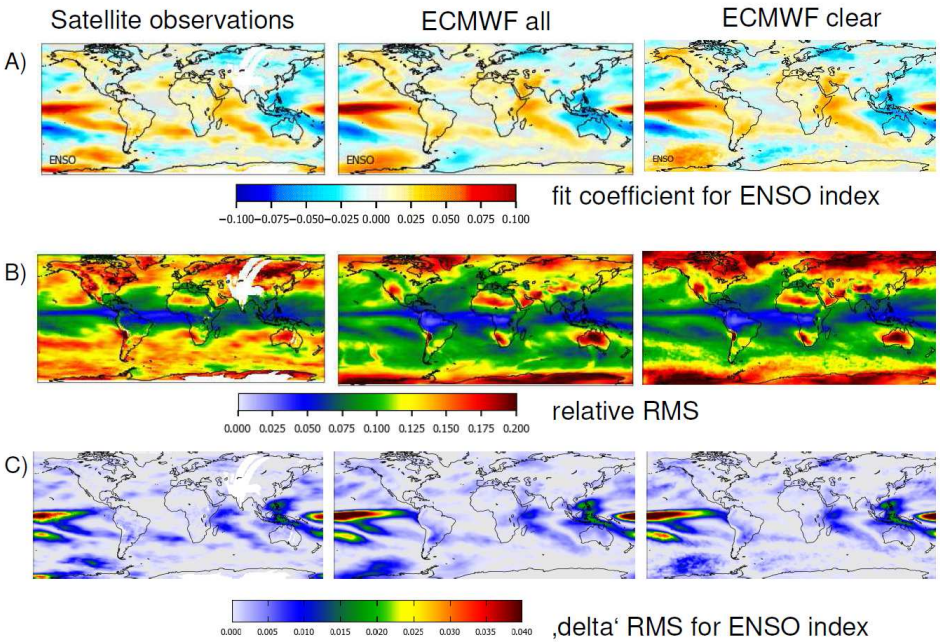

Fig. ~~5~~4: Global maps with the ENSO fit results for the three TCWV data sets. A) Fit coefficients; B) RMS of the differences between original data sets and fit functions; C) delta RMS values which describe the relative difference of the RMS if the ENSO index is included ~~of~~ or excluded in the fit function (for details see text).

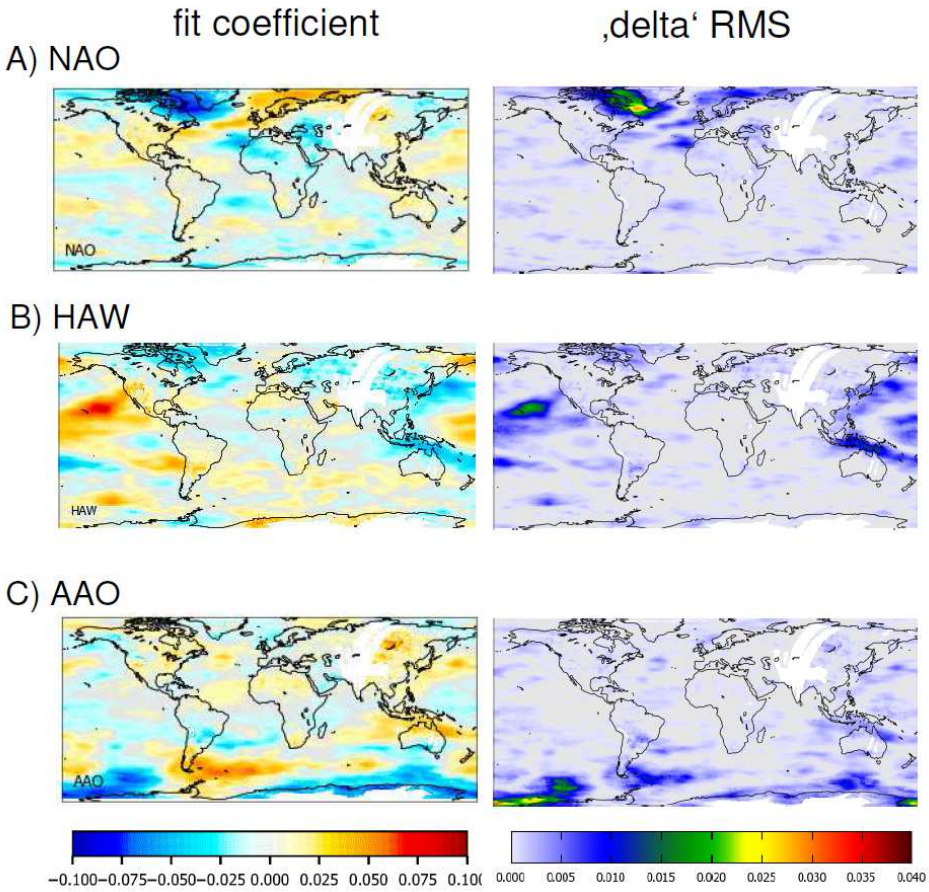

Fig. 65: Global maps with the fit results (right) and delta RMS (left) for selected teleconnection indices with activity centers in northern high latitudes (A), Subtropics (B) and southern high latitudes (C). Results for the TCWV data set from satellite observations.

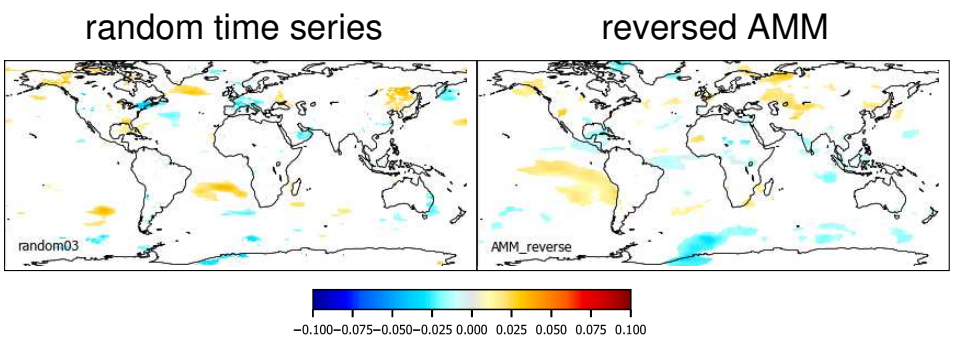

Fig. 6 Global maps of the fit results for an artificial time series containing only white noise (left) and a temporally reversed teleconnection index (AMM, right). The white areas represent fit results, that are classified as non-significant by the fit routine (for a 5% significance level).

Formatiert

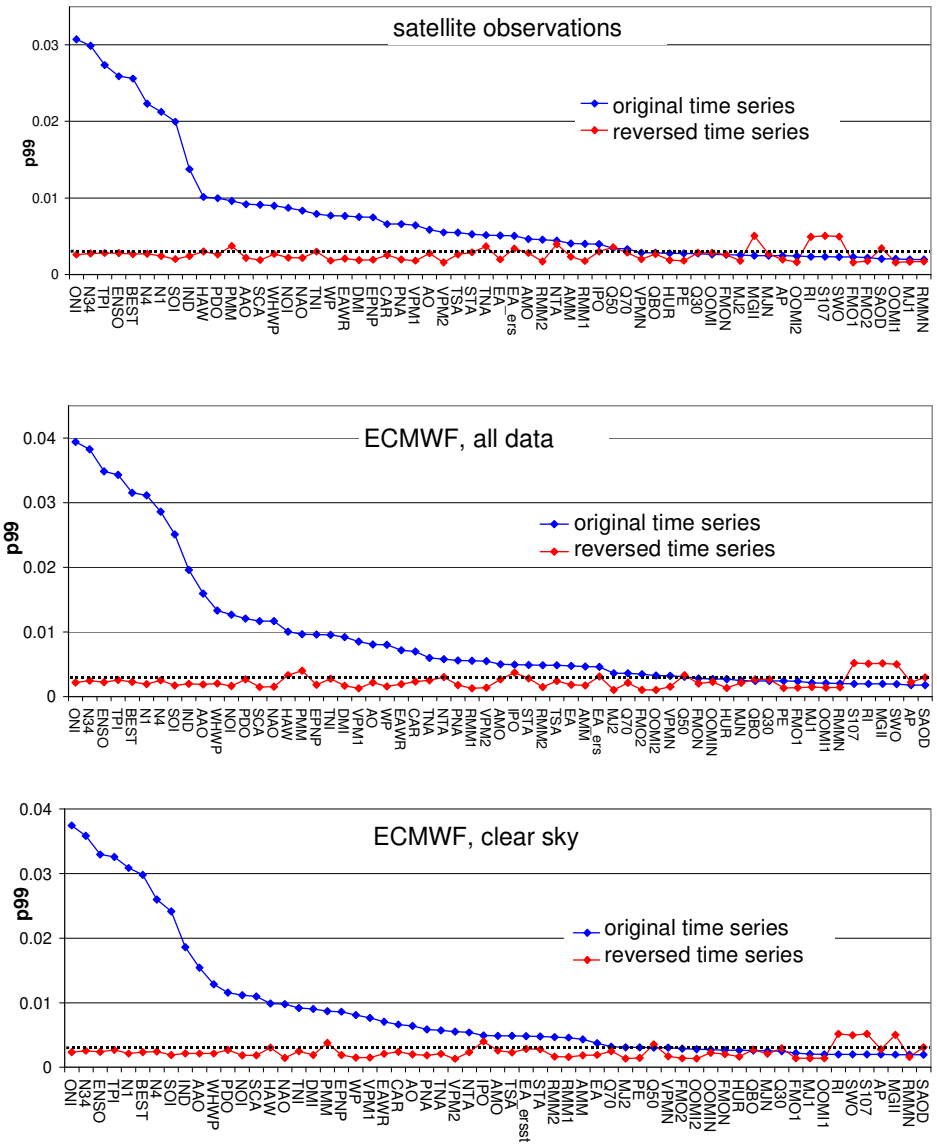

Fig. 7: Blue markers: 99th percentiles (p99) of the delta RMS of the original indices for the three TCWV data sets. Red markers: similar results for the temporally reversed indices. Black lines: significance threshold. The indices are sorted from highest to lowest p99 values for the original indices.

1580

1585

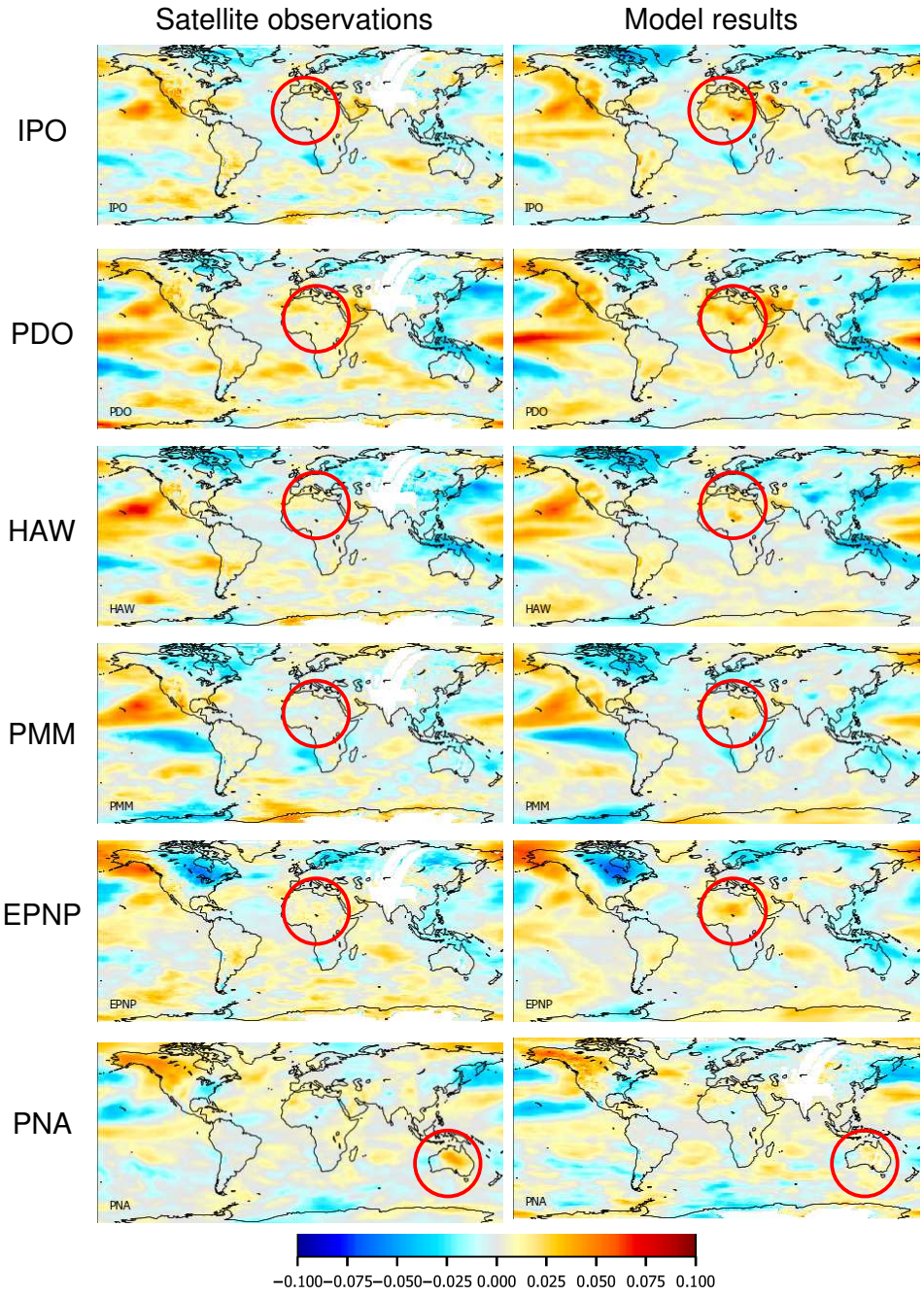

Fig. 8: Fit coefficients for selected teleconnection indices, for which different patterns were found in the TCWV data set from satellite observations (left) and model simulations (right). The red circles indicate regions with substantial differences between the results for both data sets.

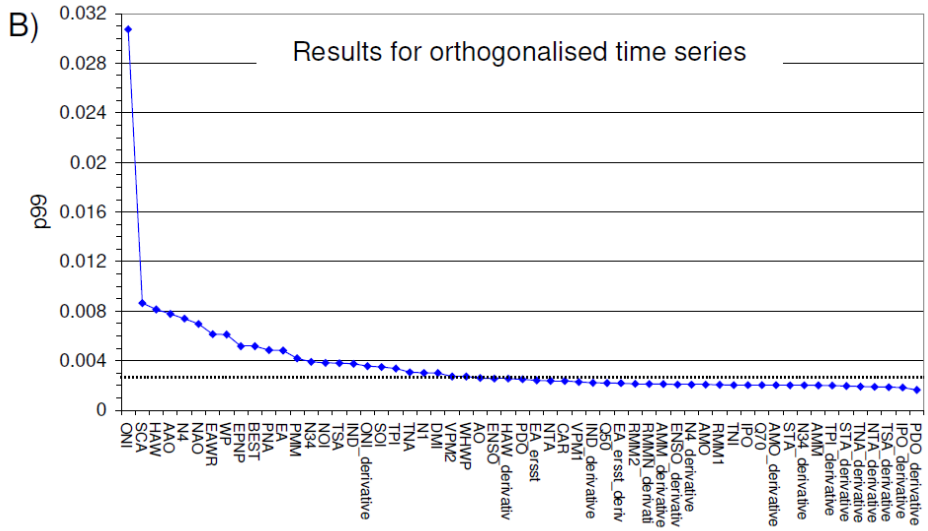

Fig. 9. The 99th percentiles (p99) of the delta RMS of the ~~derivatives of the indices (A) and the~~ orthogonalised indices ~~(B)~~. The black lines represent the significance threshold. The indices are sorted from highest to lowest p99 values.

A) Significant original indices satellite

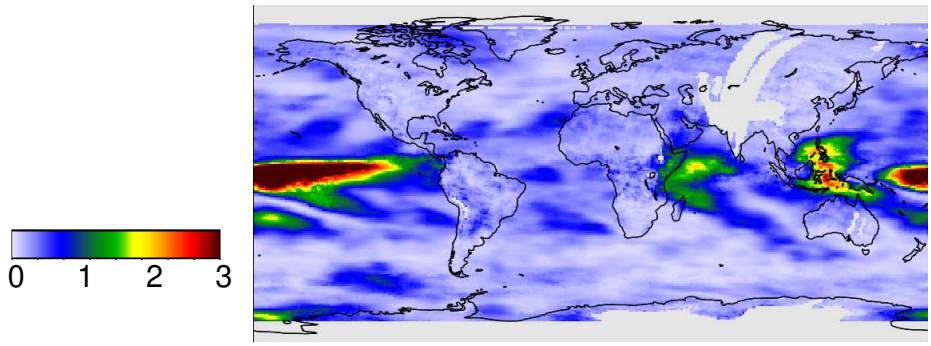

B) Significant orthogonalised indices satellite

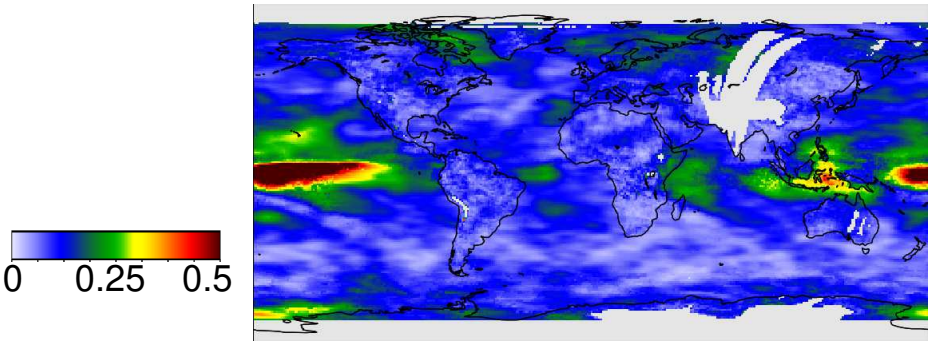

C) Significant orthogonalised indices ECMWF

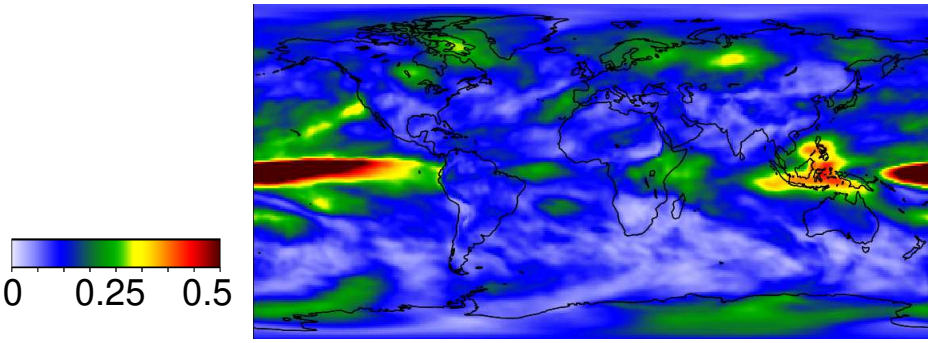

Fig. 10: Cumulative delta RMS for different selections of indices and data sets (note the different colour scales).

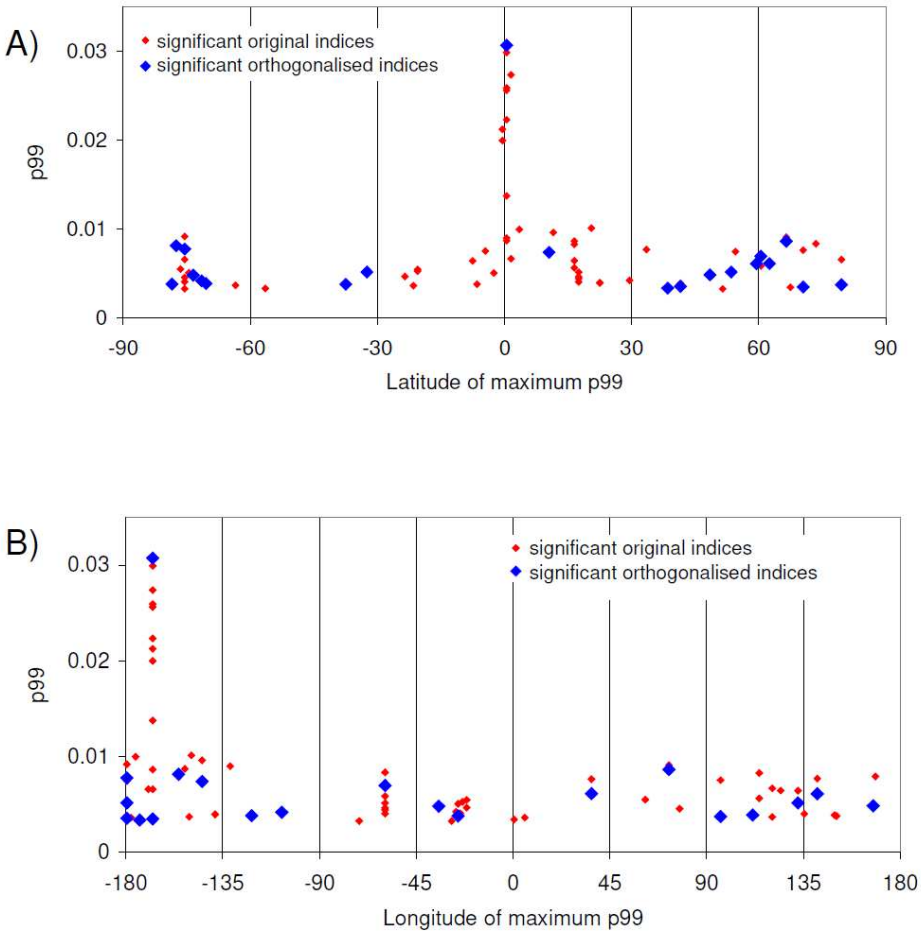

Fig. 11: Location of the 99th percentile of the delta RMS values detected in the TCWV data derived from satellite observations as function of latitude (A) or longitude (B). Red points indicate results for the original indices, blue points for the orthogonalised indices.

Appendix 1

Normalisation of the delta RMS values

In many teleconnection studies (e.g. Horel, 1981 and references therein), the strength of a teleconnection index is quantified by calculating the ratio of the difference of the RMS (with and without an index included) and the total RMS. In this study we applied a different procedure, because the total RMS depends on many factors, in particular also on the uncertainties of the considered data set. Since we want to compare the delta RMS values derived for different data sets (in particular the TCWV data sets derived from satellite observations and model results, but also other datasets) in a quantitative way, we decided to divide the RMS (with and without an index included) by the zonal mean of the considered data set. Thus the delta RMS shows the relative impact of the respective index. While the RMS of the different TCWV data sets are rather different (see Fig. 4, middle panel), the zonal means are very similar (Fig. 2). The zonal mean was chosen (instead of the long term average of each considered 1° x 1° pixel), because for some data sets used in this study (especially the wind data sets) large variations and even zero-crossings exist, which would lead to meaningless delta-RMS values. We compared the delta RMS values calculated by our new definition with those of the more traditional definition for the TCWV data sets (Fig. A1). The obtained global patterns of both delta RMS definitions are almost identical.

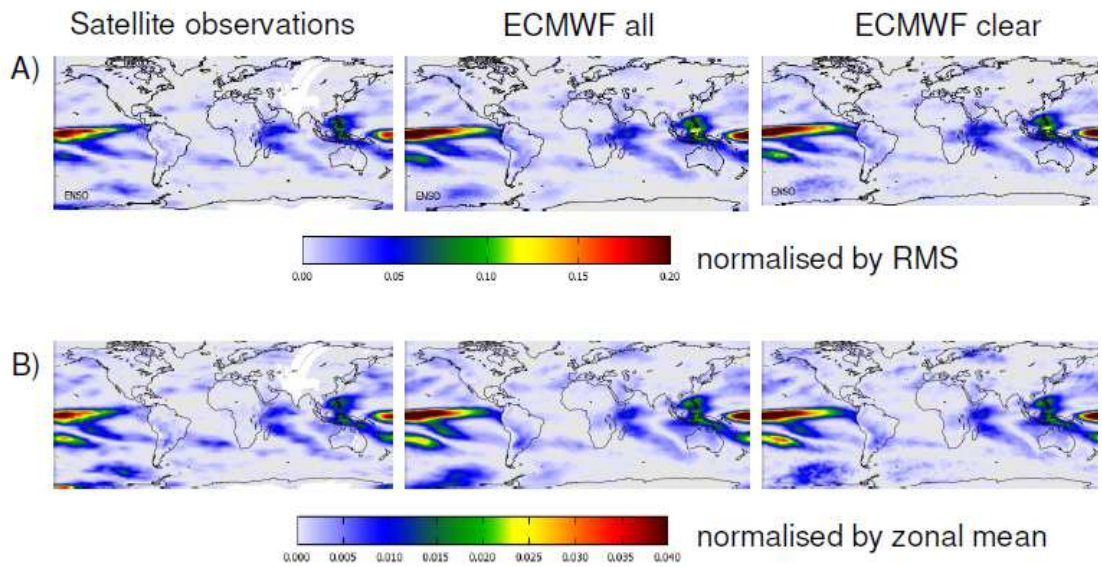

Fig. A1: Comparison of delta RMS values for the ENSO index calculated in two different ways. A) The difference of the RMS with and without the ENSO index included in the fit is divided by the respective RMS of each 1°x1° pixel; B) The difference of the RMS with and without the ENSO index included in the fit is divided by the zonal mean of the TCWV at the same latitude. Note the different colour scales.

Appendix ~~1~~ 2

Effect of the temporal correlation of the reversed indices with the original indices

For several temporally reversed indices, the ~~The~~ 99th percentiles in Fig. 7 are substantially higher ~~for several reversed indices~~ than for others. Since all reversed indices represent non-geophysical variations, such enhanced 99th percentiles are not expected. Thus this finding was further investigated. It turned out that the enhanced values are caused by accidental correlations of these reversed indices with original indices (see Fig. ~~A6~~A2), for which high 99th percentile values are found. This reasoning is confirmed by the results shown in Fig. ~~A7~~A3. There, high p99 values for reversed indices are always found if they are correlated with original indices with high p99 values. To avoid the effects of such accidental enhanced p99 values, only the reversed indices with no obvious correlations with original indices with high p99 values were kept for further processing (red boxes in Fig. ~~A6~~A3). Here it should be noted that two somehow arbitrary choices were made:

a) the selection of the selected reversed indices (red boxes in Fig. ~~A6~~A3) was made by visual inspection.

b) the ~~influence~~ effect of the correlation of the reversed indices with the original indices was only investigated for the 8 original indices with the highest p99 values.

Fortunately, both choices had only a minor influence on the derived threshold value. With respect to the first point, it should be noted that while the selection was made rather conservatively, still many reversed indices were kept after the filtering process. It was also found that most of the skipped reversed indices were ~~skipped~~ removed because of enhanced correlations with several original indices. With respect to the second point it should be noted that it makes sense to consider only the original indices with the highest p99 values, because the correlations of the reversed indices with the original indices are in general rather low (see Fig. ~~A6~~A2). The p99 values of the selected 8 original indices with the highest p99 values are in general substantially higher than the p99 values of the remaining indices. In sensitivity studies we found that taking account more than 8 original indices had a negligible effect on the derived threshold values.

The red markers in Fig. A4~~7~~ represent the p99 values for the indices which were kept after applying the selection criteria explained above. In the final step, from these p99 values the average and standard deviation are calculated. The p99 threshold for the significance of a indices is then calculated as the sum of the average plus three times the standard deviation (for the TCWV data set from satellite observations the threshold is: 0.00200 + 3*0.00036 = 0.00309). This procedure was chosen, because the threshold values calculated in this way are very close to the maximum p99 values of the remaining indices (red dots in Fig. A4~~7~~) but are hardly affected by possible remaining outliers. The derived threshold value is indicated by the dashed black line in Fig. 7.

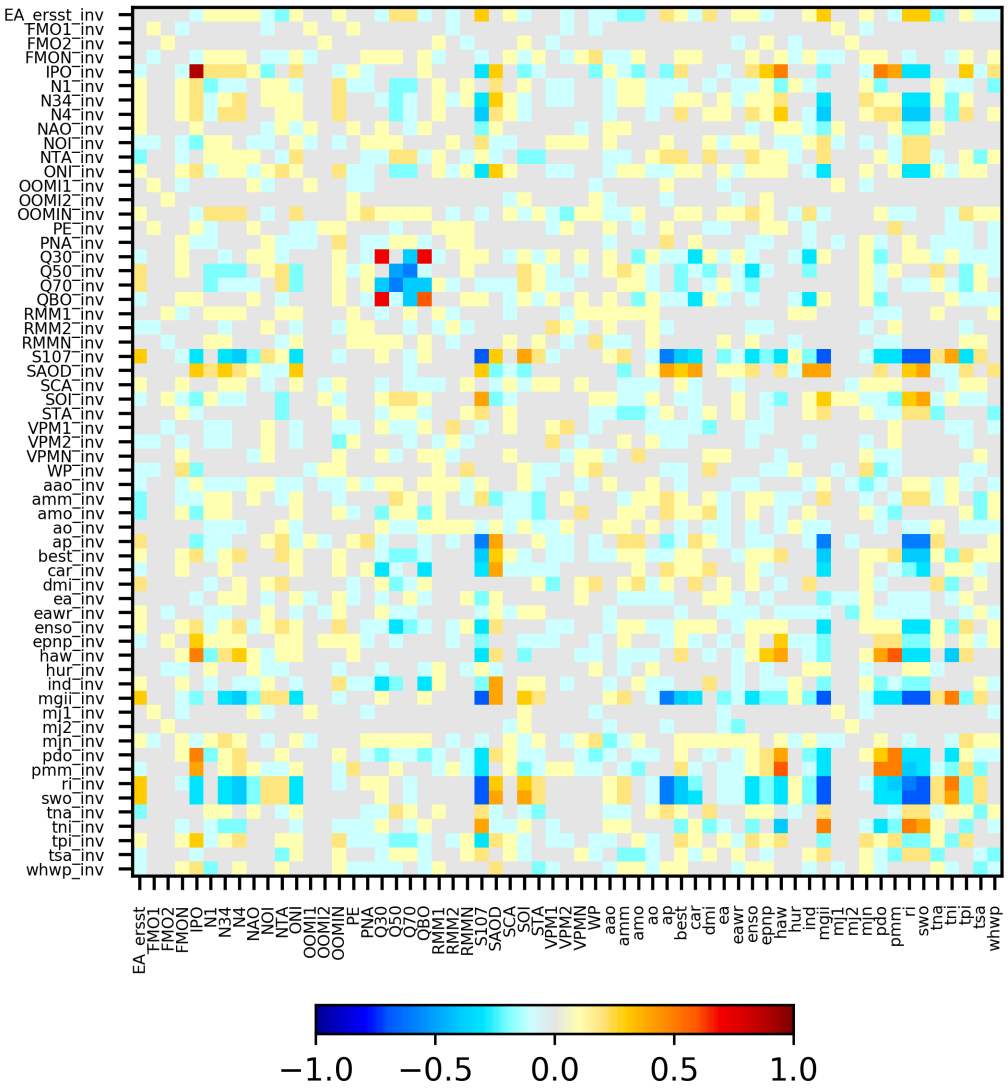

1745 **Fig. A2: Correlation coefficients between the temporally reversed and original indices. For several combinations enhanced coincidental correlations are found.**

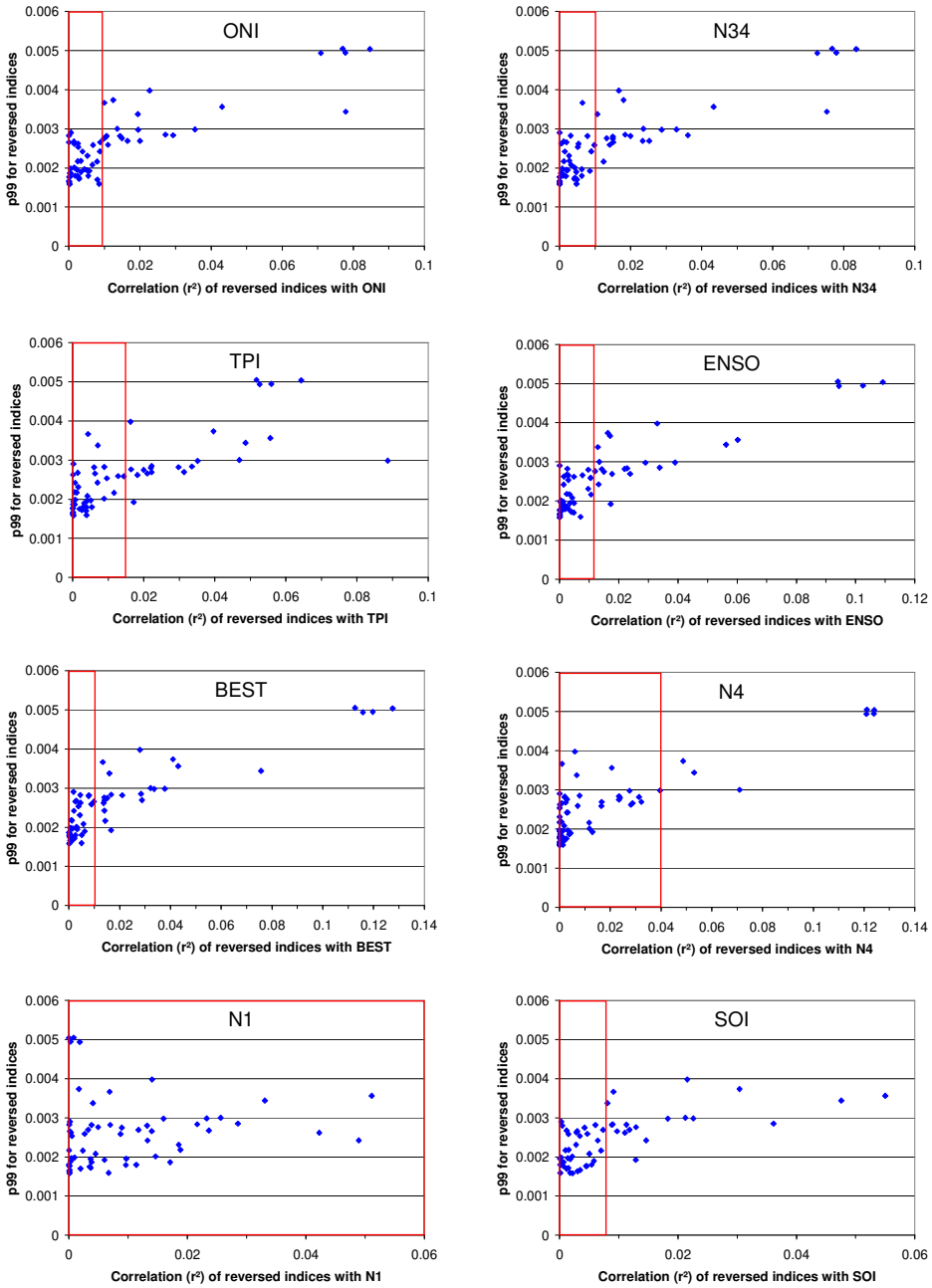

Fig. A3: Correlation plots for the 8 original indices with the highest p99 values. The blue dots represent the 61 reversed indices. The x-axis describes the correlation coefficients of the reversed indices with the selected original indices. The y-axis describes the p99 value or the reversed indices. High p99 values are found for the reversed indices which show high correlation to the original indices.

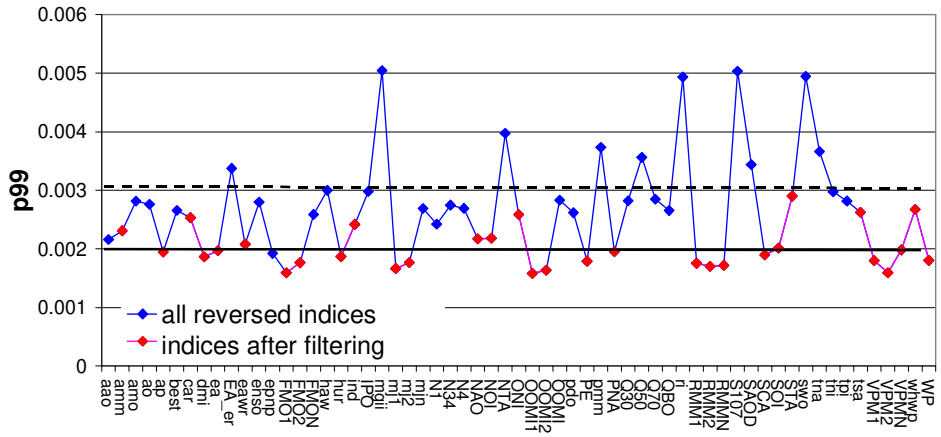

Fig. A4: The 99th percentiles (p99) of the delta RMS of the temporally reversed indices for the TCWV from satellite observations (same as in Fig. 7, top). The blue markers indicate indices which are excluded from the calculation of the significance threshold (for details see text).

Appendix A3

Effect of a time shift of the teleconnection indices

In addition to the p99 values themselves, also the effect of time shifts $\Delta t = \pm 1$ month of the indices on the p99 values was considered to decide whether an index was significantly identified in a global data set, because for indices with a geophysical relationship to a considered data set, the exact temporal synchronisation should be important (but might depend on region). In contrast, for indices without a geophysical relationship to the considered data set, the p99 values should not depend on the exact temporal synchronisation. Here it should be noted that for some teleconnections, also time lags might exist between the corresponding indices and the atmospheric variables. Thus the lack of an exact synchronization should not be seen as a strong indication that the corresponding teleconnection was not significantly detected in a global data set. But conversely, if a clear synchronisation for a teleconnection is found, this can be interpreted as a a strong indication for significant detection.

In Fig. A5 the p99 values for the original and shifted (by ± 1 month) indices are shown for the TCWV data set from satellite observations. For most data sets (especially for those with high p99 values) indeed smaller p99 values are found for the shifted indices. Here it is interesting to note that in general a stronger effect is found for atmospheric indices than for oceanic indices, which can be understood by the higher frequencies of the atmospheric indices. For several oceanic indices, even higher values are found for the shifted indices indicating a time shift (mostly a time lag) between the TCWV and these indices. For one index (AMM) higher p99 values are even found for shifts in both directions indicating an ambiguity in the synchronisation between the TCWV and the AMM index.

Another interesting finding is that for some atmospheric indices with p99 values below the significance threshold (PE, MJ2, OOMI2, FMO1) still rather small ratios of the shifted and original indices are found indicating that these indices are also probably significantly detected in the TCWV data set. Thus in the following we consider also indices with p99 values below the significance threshold but with p99 ratios below 0.8 for both shifts as significantly detected. Here it should be noted that the choice of the threshold value of 0.8 is somehow arbitrary. It was chosen because a deviation of 20% from unity is larger than the 'noise level' of the ratio. The exact choice of the threshold has only a small effect on the obtained results.

Formatiert

Formatiert: Nicht Hervorheben

Formatiert: Nicht Hervorheben

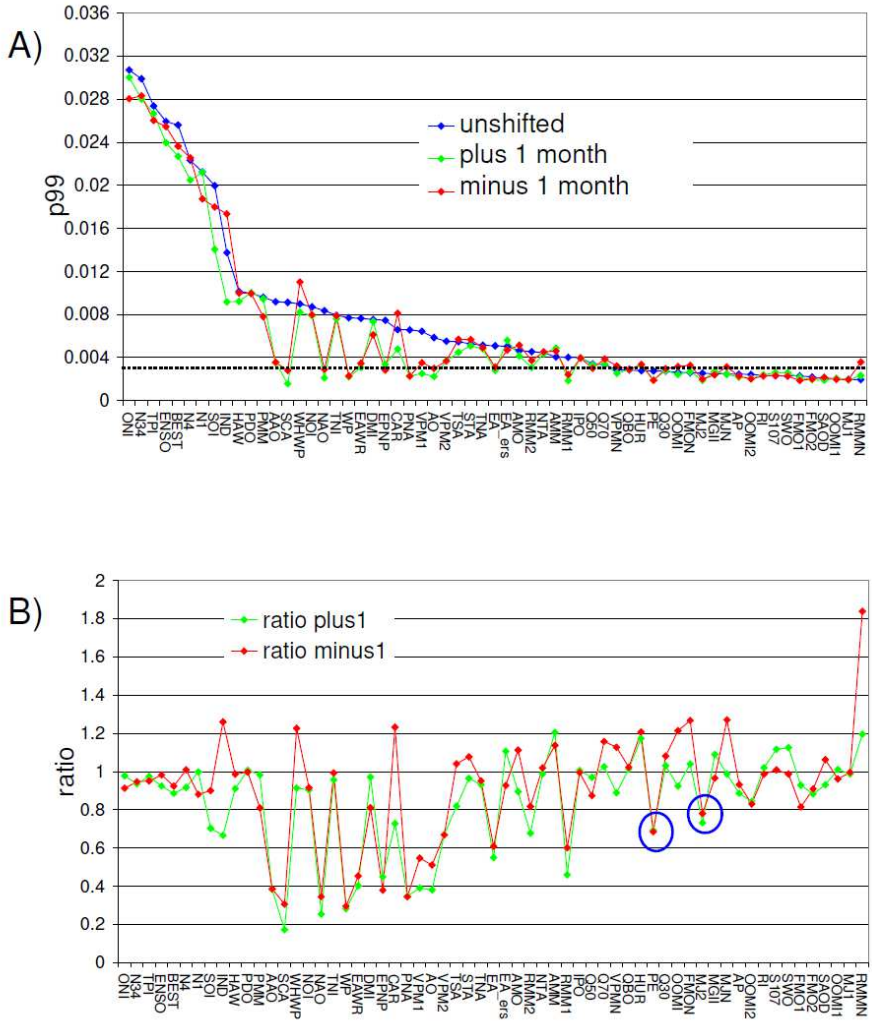

Fig. A5: Top: 99th percentiles (p99) of the delta RMS values for the original (blue) and shifted indices (green: plus 1 month; red: minus 1 month). The indices are sorted from highest to lowest p99 values for the unshifted original indices. Bottom: ratios of the p99 values of the shifted and original indices. Results are for the TCWV data set from satellite observations. The blue circles indicate teleconnection indices with p99 values below the threshold, but ratios of the shifted indices < 0.8.

Appendix ~~2~~ 4

Additional Figures and tables

Name (data source)	Short name	Type	Indices 1995 - 2015
A) Indices similar to ENSO			
Multivariate ENSO Index (NOAA)	ENSO	Oceanic & Atmospheric	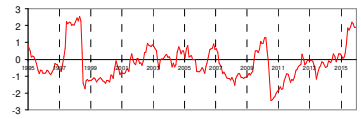
Bivariate ENSO Timeseries (NOAA)	BEST	Oceanic & Atmospheric	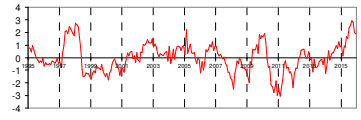
Oceanic Nino Index (NOAA)	ONI	Oceanic	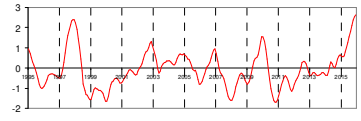
Nina 3.4 (NOAA)	N34	Oceanic	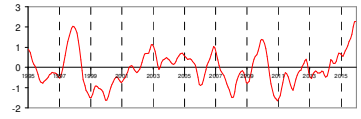
Nina 4 (NOAA)	N4	Oceanic	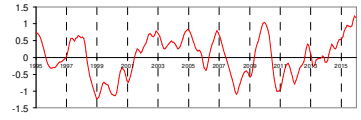
Tripole Index for the Interdecadal Pacific Oscillation (NOAA)	TPI	Oceanic	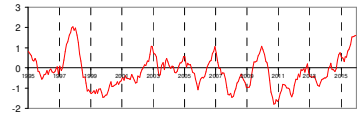
Indian Ocean Index (NOAA)	IND	Oceanic	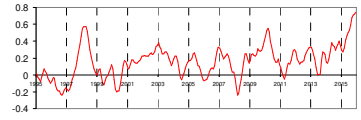
B) Oceanic indices			
Nina 1 + 2 (NOAA)	N1	Oceanic	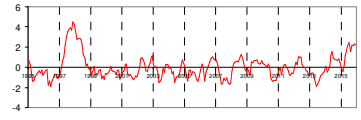
Pacific Decadal Oscillation (NOAA)	PDO	Oceanic	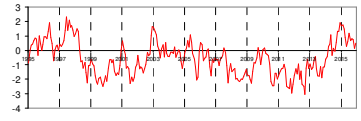
Interdecadal Pacific Oscillation (Ministry of environment, NZ)	IPO	Oceanic	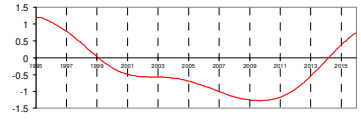

Formatiert

Western Hemisphere warm pool (NOAA)	WHWP	Oceanic	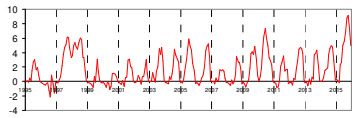
North Tropical Atlantic (NOAA)	NTA	Oceanic	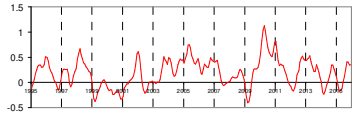
Tropical Northern Atlantic (NOAA)	TNA	Oceanic	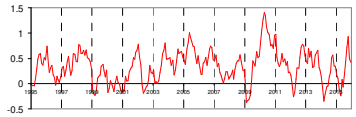
South Tropical Atlantic (NOAA)	STA	Oceanic	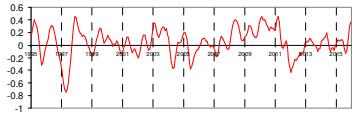
Tropical Southern Atlantic (NOAA)	TSA	Oceanic	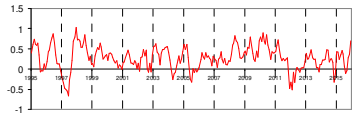
Equatorial Atlantic Index (NOAA)	EA_ersst	Oceanic	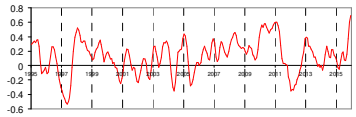
Caribbean Index (NOAA)	CAR	Oceanic	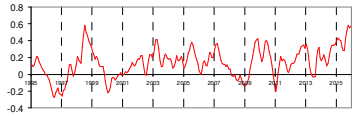
Atlantic Meridional Mode (NOAA)	AMM	Oceanic	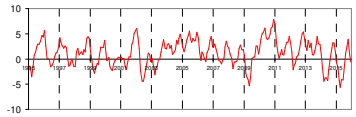
Pacific Meridional mode (University of Wisconsin, USA)	PMM	Oceanic	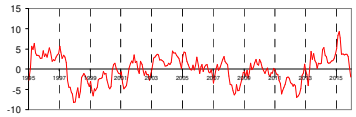
Atlantic multidecadal Oscillation (NOAA)	AMO	Oceanic	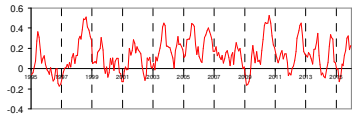
Hawaiian Index (NOAA)	HAW	Oceanic	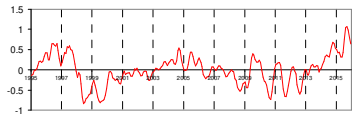
Dipole Mode Index (NOAA)	DMI	Oceanic	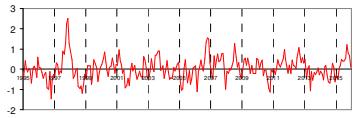

Trans-Nino index (NOAA)	TNI	Oceanic	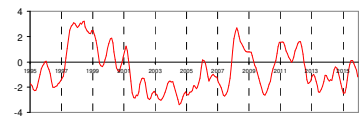
C) Atmospheric indices (except MJO indices)			
Southern Oscillation Index (NOAA)	SOI	Atmospheric	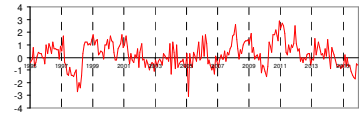
Northern Oscillation Index (NOAA)	NOI	Atmospheric	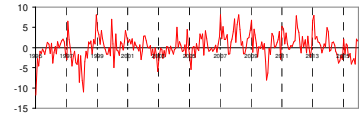
North Atlantic Oscillation (NOAA)	NAO	Atmospheric	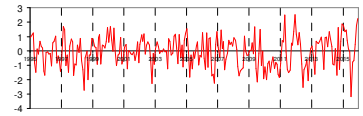
Pacific/North American pattern (NOAA)	PNA	Atmospheric	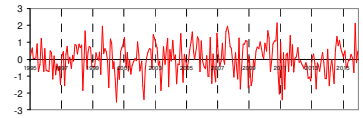
East Atlantic pattern (NOAA)	EA	Atmospheric	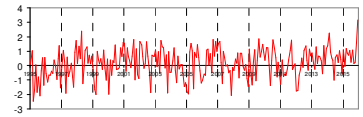
East Atlantic/Western Russia pattern (NOAA)	EAWR	Atmospheric	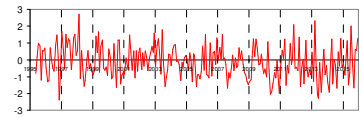
Scandinavia pattern (NOAA)	SCA	Atmospheric	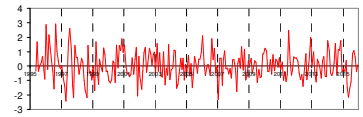
West Pacific pattern (NOAA)	WP	Atmospheric	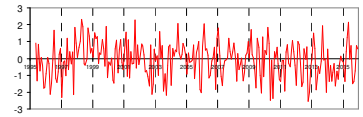
East Pacific/North Pacific pattern (NOAA)	EPNP	Atmospheric	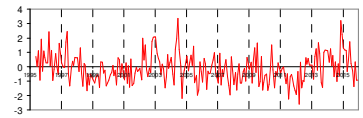
Polar-Eurasian pattern (NOAA)	PE	Atmospheric	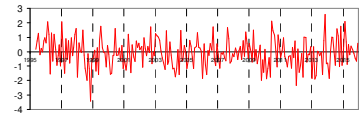

Formatiert

Arctic Oscillation (NOAA)	AO	Atmospheric	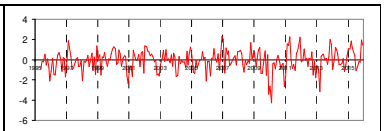
Antarctic Oscillation (NOAA)	AAO	Atmospheric	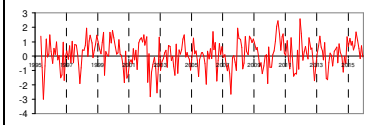
Quasi-Biennial Oscillation at 30 hPa (NOAA)	QBO	Atmospheric	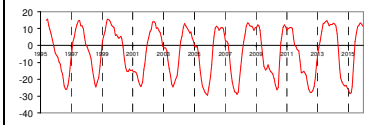
Quasi-Biennial Oscillation at 30 hPa (Free University of Berlin)	Q30	Atmospheric	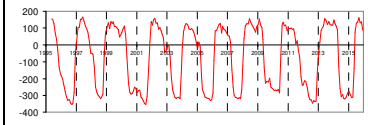
uasi-Biennial Oscillation at 50 hPa (Free University of Berlin)	Q50	Atmospheric	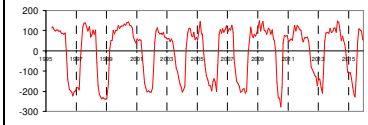
uasi-Biennial Oscillation at 70 hPa (Free University of Berlin)	Q70	Atmospheric	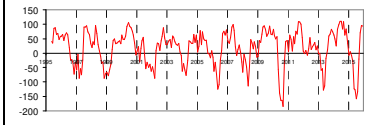
D) MJO Indices*			
Madden Julian Oscillation (OMI) Component 1 (NOAA)	MJ1	Atmospheric	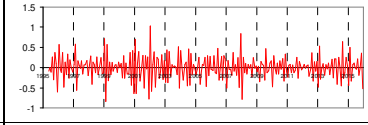
Madden Julian Oscillation (OOMI) Component 1 (NOAA)	OOMI1	Atmospheric	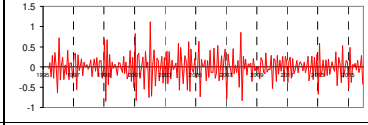
Madden Julian Oscillation (FMO) Component 1 (NOAA)	FMO1	Atmospheric	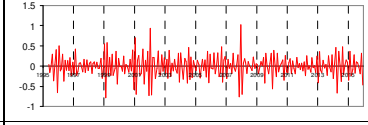
Madden Julian Oscillation (VPM) Component 1 (NOAA)	VPM1	Atmospheric	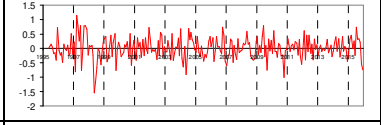
Madden Julian Oscillation** Component 1 (Australian Bureau of Meteorology)	RMM1	Atmospheric	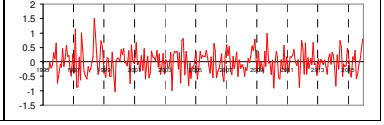

Formatiert

Madden Julian Oscillation (OMI) Component 2 (NOAA)	MJ2	Atmospheric	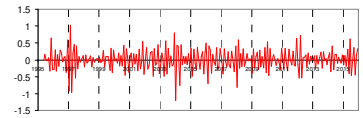
Madden Julian Oscillation (OOMI) Component 2 (NOAA)	OOMI2	Atmospheric	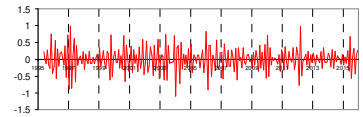
Madden Julian Oscillation (FMO) Component 2 (NOAA)	FMO2	Atmospheric	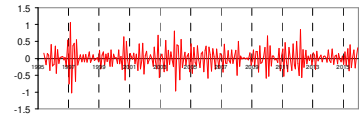
Madden Julian Oscillation (VPM) Component 2 (NOAA)	VPM2	Atmospheric	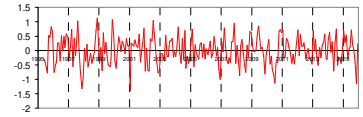
Madden Julian Oscillation** Component 2 (Australian Bureau of Meteorology)	RMM2	Atmospheric	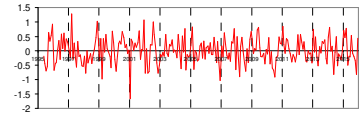
Madden Julian Oscillation (OMI) Sum of both compoenents (NOAA)	MJN	Atmospheric	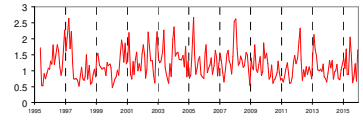
Madden Julian Oscillation (OOMI) Sum of both (NOAA)	OOMIN	Atmospheric	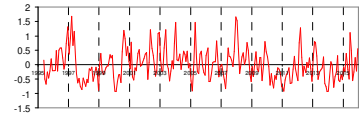
Madden Julian Oscillation (FMO) Sum of both (NOAA)	FMON	Atmospheric	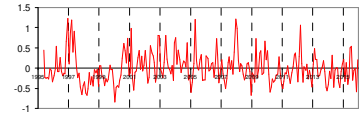
Madden Julian Oscillation (VPM) Sum of both (NOAA)	VPMN	Atmospheric	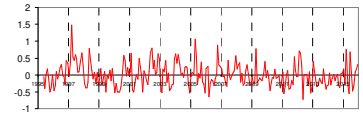
Madden Julian Oscillation** Sum of both (Australian Bureau of Meteorology)	RMMN	Atmospheric	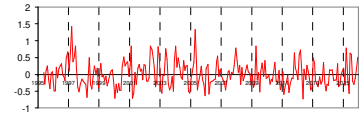
E) Other Indices			
Composite MG II index (University of Bremen)	MGII	solar	

Formatiert

Magnetic AP index (NOAA, GeoForschungsZentrum, Postdam)	AP	solar	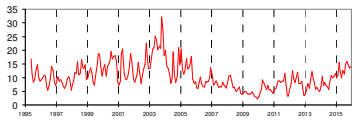
Radio flux at 10.7 cm (NOAA, Penticton, B.C., Canada)	S107	solar	
Sun spot number (NOAA, SWPC Space Weather Operations)	SWO	solar	
Sun spot number (NOAA, S.I.D.C. Brussels International Sunspot Number)	RI	solar	
Stratospheric AOD* (LATMOS/IPSL)**	SAOD	Atmospheric	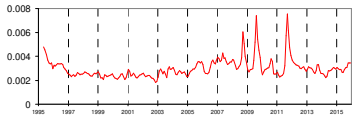
Total number of hurricanes in Atlantic region (NOAA)	HUR	Atmospheric	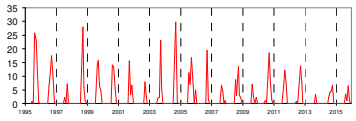

Fig. ~~A3~~A6: List of original indices used in this study. Besides the short names also the data sources and ~~figures with~~ their temporal variation from 1995 to 2016 are shown.
*All MJO indices are convoluted with a Gaussian kernel ~~fo~~ of 30 days FWHM; **Original index according to Wheeler and Hendon, 2004;
***Khaykin et al., 2017

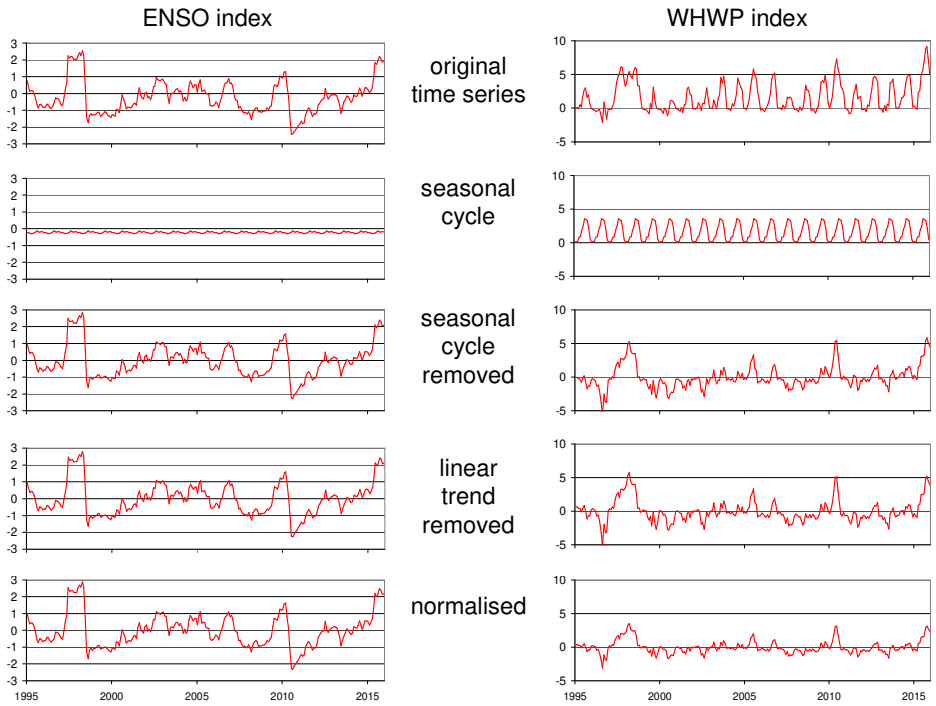

Fig. ~~3~~A7: Illustration of the preparations for the indices before they are used in the fit to the global data sets: First, the mean seasonal cycles and linear trends are subtracted. Then the differences are normalised by their standard deviations.

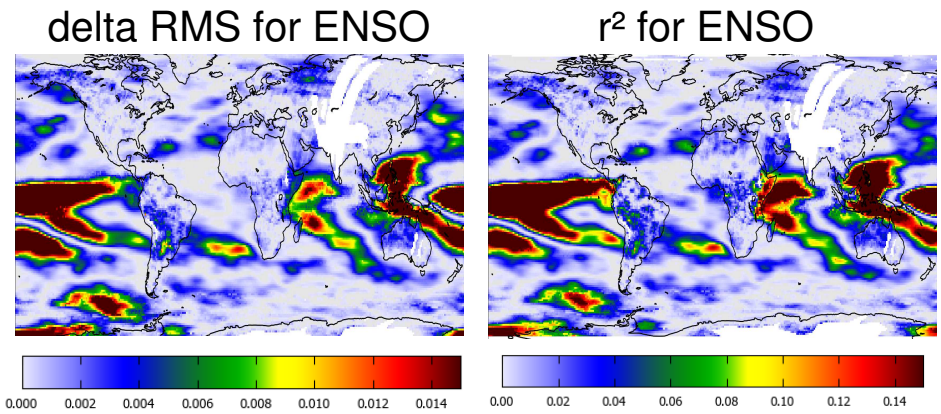

Fig. A8: Delta RMS (left) and r² values (right) for the fit of the ENSO index to the TCWV derived from satellite observations.

Formatiert: Nicht Hervorheben

Short name	Satellite observations	ECMWF data	Short name	Satellite observations	ECMWF data
Indices similar to ENSO					
ENSO	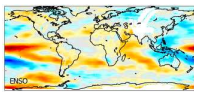	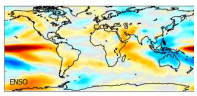	N4	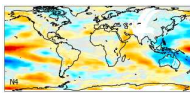	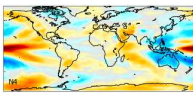
BEST	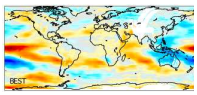	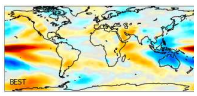	TPI	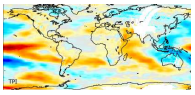	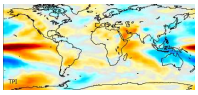
ONI	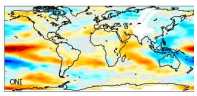	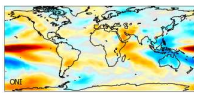	IND	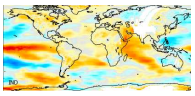	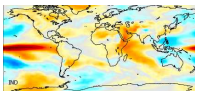
N34	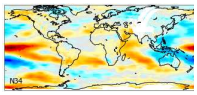	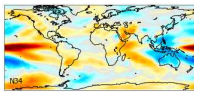			
Oceanic indices					
N1	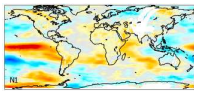	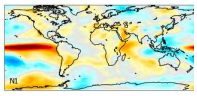	EA_ersst	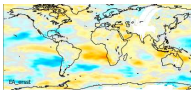	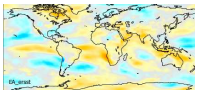
PDO	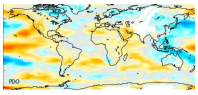	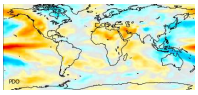	CAR	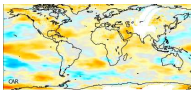	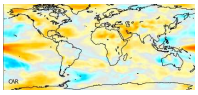
IPO	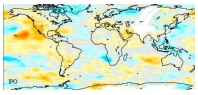	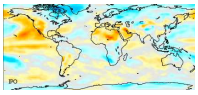	AMM	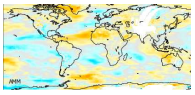	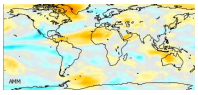
WHWP	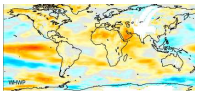	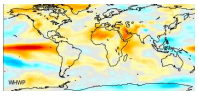	PMM	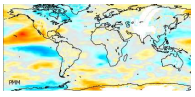	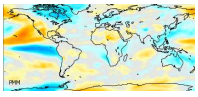
NTA	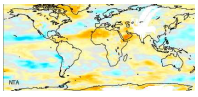	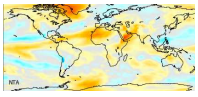	AMO	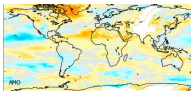	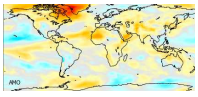
TNA	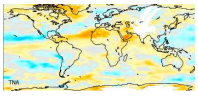	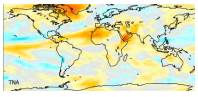	HAW	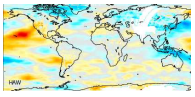	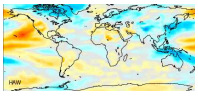
STA	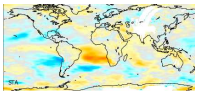	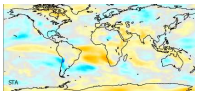	DMI	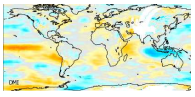	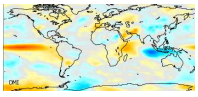
TSA	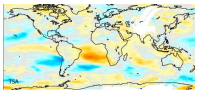	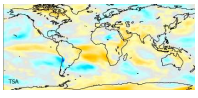	TNI	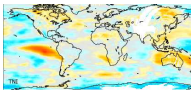	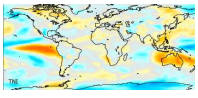
Atmospheric Indices					
SOI	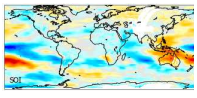	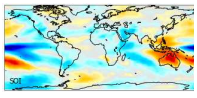	EPNP	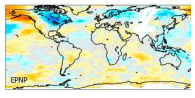	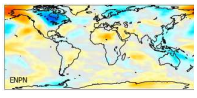

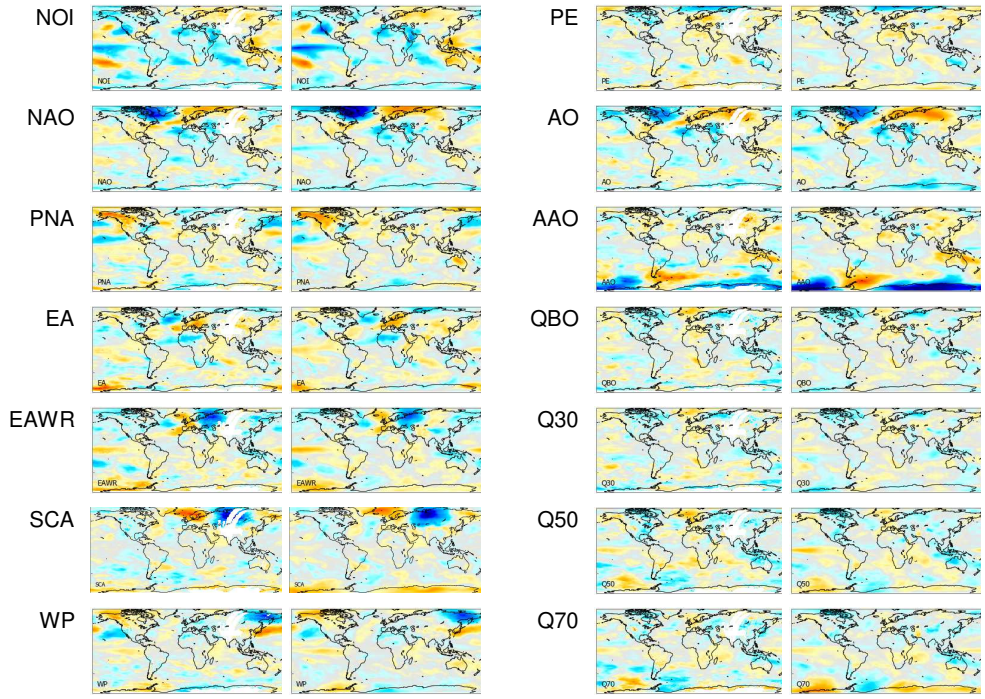
NOI
PE
NAO
AO
PNA
AAO
EA
QBO
EAWR
Q30
SCA
Q50
WP
Q70

MJO Indices

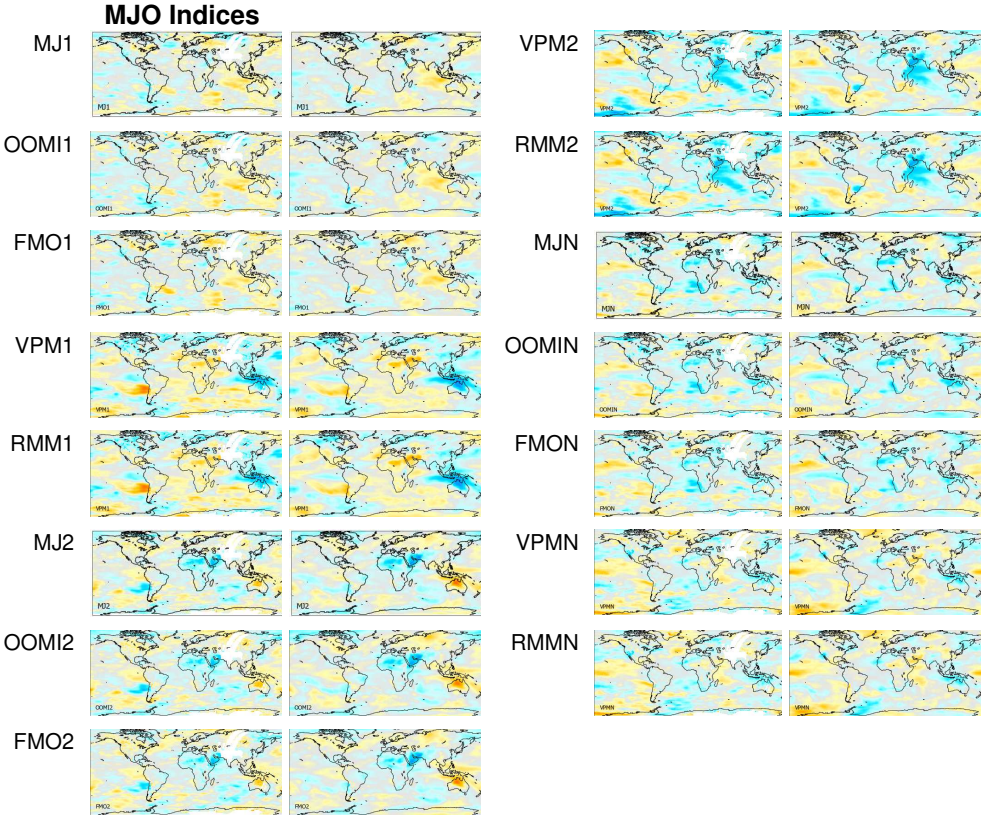
MJ1
VPM2
OOMI1
RMM2
FMO1
MJN
VPM1
OOMIN
RMM1
FMON
MJ2
VPMN
OOMI2
RMMN
FMO2

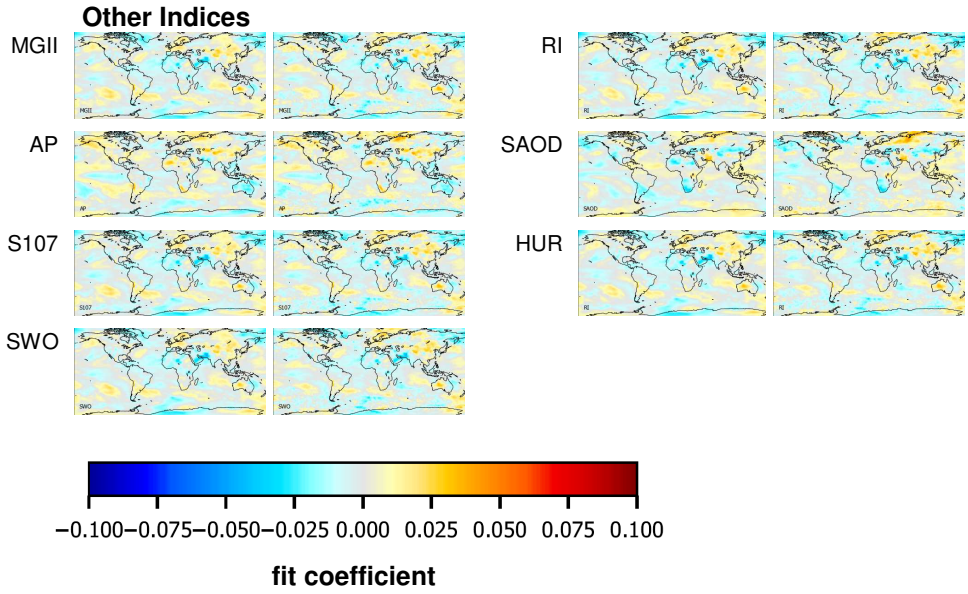

Fig. ~~A4~~A9: Fit coefficients ~~(top) and delta RMS values (bottom)~~ for all indices used in this study. Shown are the results for the TCWV data set from satellite observations (left) and model results (for all sky conditions) ~~three water vapor data sets: satellite observations (left), model results (center), and model results for clear sky conditions~~ (right).

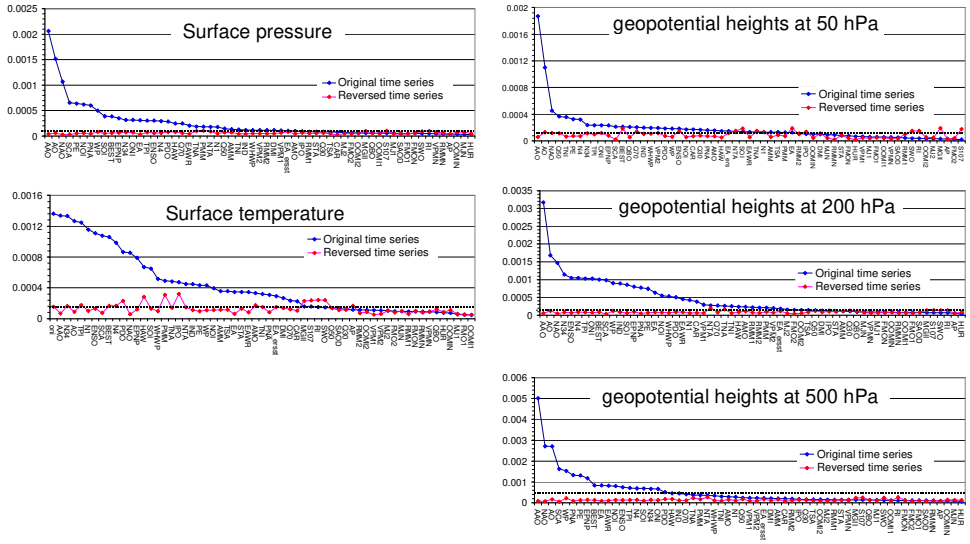

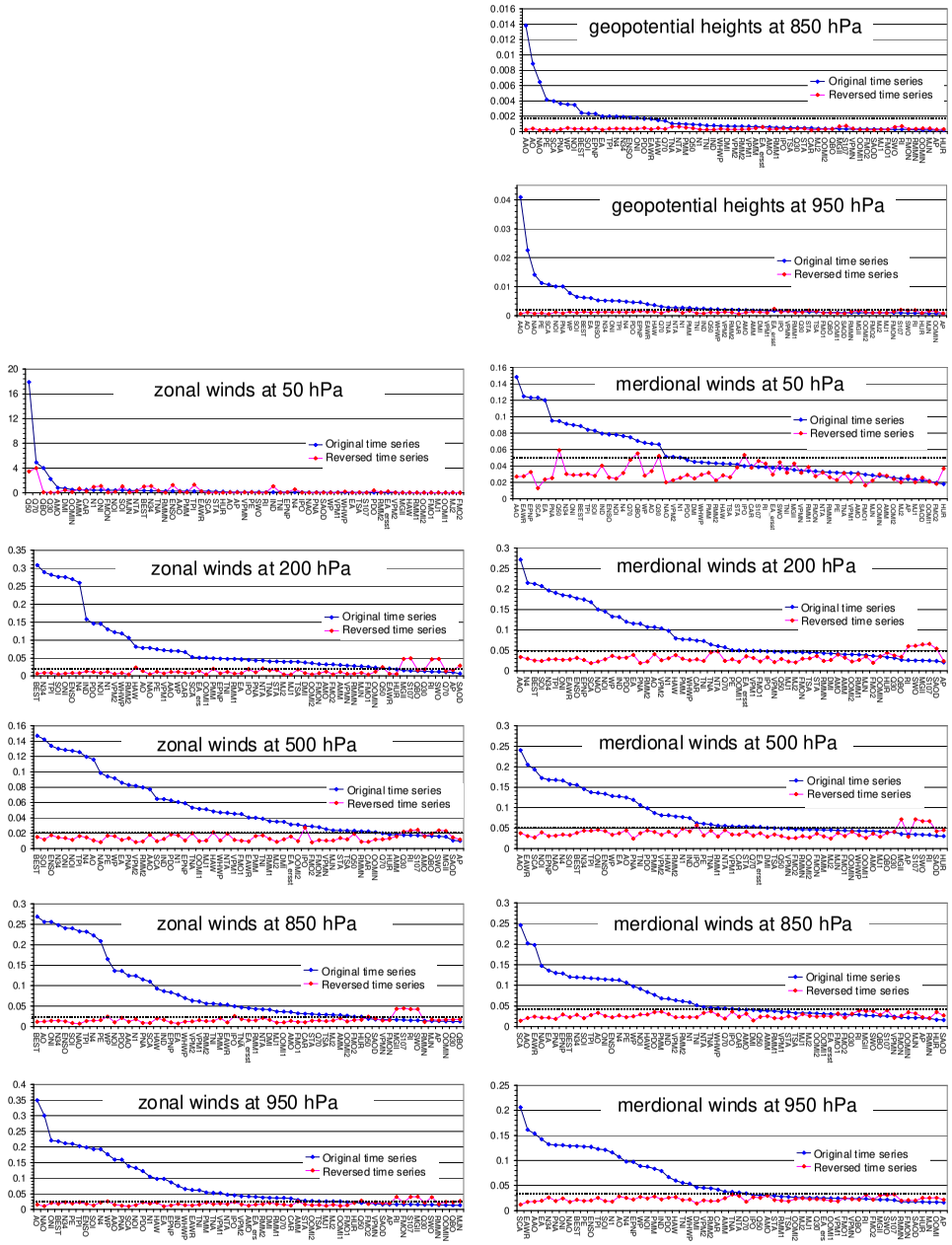

Fig. A9A10: 99th percentiles of the delta RMS values (p99) found for the different indices in different global data sets. Blue markers: p99 for the original indices; red markers: p99 for the temporally reversed indices; black lines: significance thresholds. The indices are sorted from highest to lowest p99 values for the original indices.

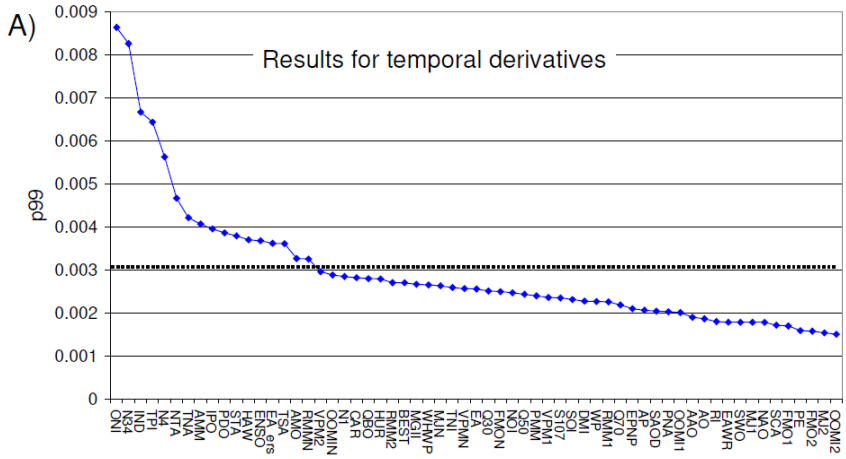

1885 **Fig. A11. The 99th percentiles (p99) of the delta RMS of the derivatives of all indices. The black lines represent the significance threshold. The indices are sorted from highest to lowest p99 values.**

1890

1895

1900

1905

1910

1915

1920

1925

1930

	Original indices	Orthogonalised indices
1	ONI	
2	SCA	SCA ortho
3	HAW	HAW ortho
4	AAO	AAO ortho
5	N4	N4 ortho
6	NAO	NAO ortho
7	EAWR	EAWR ortho
8	WP	WP ortho
9	EPNP	EPNP ortho
10	BEST	BEST ortho

	Original indices	Orthogonalised indices
11	PNA	PNA ortho
12	EA	EA ortho
13	PMM	PMM ortho
14	N34	N34 ortho
15	NOI	NOI ortho
16	TSA	TSA ortho
17	IND	IND ortho
18	ONI derivative	ONI derivative ortho
19	SOI	SOI ortho
20	TPI	TPI ortho

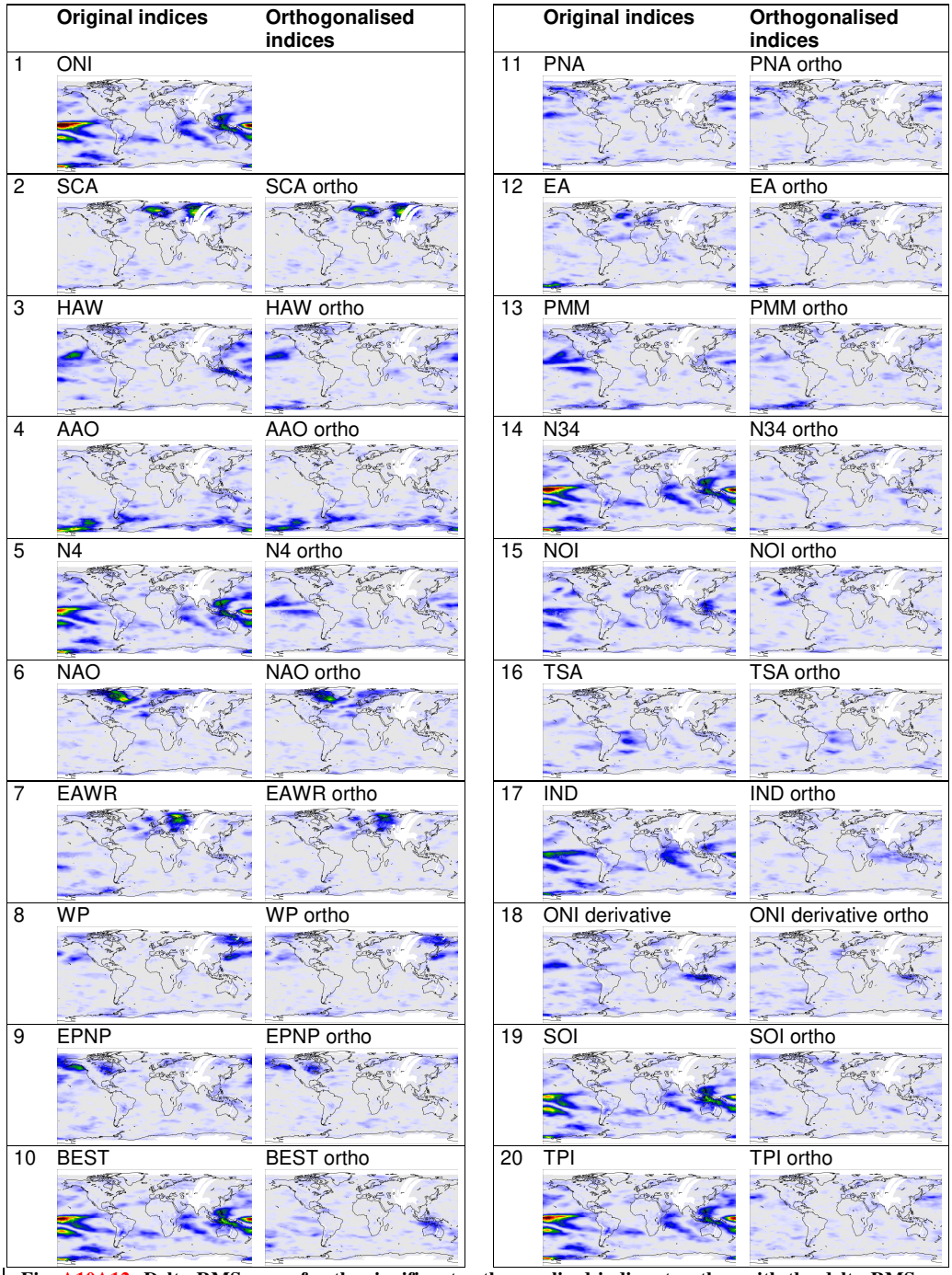

Fig. ~~A10~~A12: Delta RMS maps for the significant orthogonalised indices together with the delta RMS maps for the original indices. The numbers at the left sides indicate the order (descending) of the p99 values (see also Fig. 89).

1935

1940 **Table A1 Significant indices for all data sets (indices with p99 values below threshold but shift ratios <0.8 are indicated in brackets).**

Data set	Number of significant indices	Significant indices (from highest to lowest p99 values)
TCWV sat	42 (2)	ONI, N34, TPI, ENSO, BEST, N4, N1, SOI, IND, HAW, PDO, PMM, AAO, SCA, WHWP, NOI, NAO, TNI, WP, EAWR, DMI, EPNP, CAR, PNA, VPM1, AO, VPM2, TSA, STA, TNA, EA, EA_ersst, AMO, RMM2, NTA, AMM, RMM1, IPO, Q50, Q70 (PE, MJ2)
TCWV ERA	44 (1)	ONI, N34, ENSO, TPI, BEST, N1, N4, SOI, IND, AAO, WHWP, NOI, PDO, SCA, NAO, HAW, PMM, EPNP, TNI, DMI, VPM1, AO, WP, EAWR, CAR, TNA, NTA, PNA, RMM1, VPM2, AMO, IPO, STA, RMM2, TSA, EA, AMM, EA_ersst, MJ2, Q70, FMO2, OOMI2, VPMN, Q50 (PE)
TCWV ERA clear	42 (3)	ONI, N34, ENSO, TPI, N1, BEST, N4, SOI, IND, AAO, WHWP, PDO, NOI, SCA, HAW, NAO, TNI, DMI, PMM, EPNP, WP, VPM1, EAWR, CAR, AO, PNA, TNA, VPM2, NTA, IPO, AMO, TSA, EA_ersst, STA, RMM2, RMM1, AMM, EA (PE, FMO2, OOMI2)
Tsurf	37 (1)	ONI, AAO, N34, AO, TPI, N1, ENSO, SCA, BEST, N4, PDO, NAO, EPNP, HAW, SOI, WHWP, PMM, TNA, IPO, NTA, IND, PE, WP, NOI, AMM, TSA, EA, STA, EAWR, AMO, TNI, PNA, EA_ersst, DMI, Q70, CAR (RMM2)
Spred	35 (1)	AAO, AO, NAO, SCA, PE, NOI, PNA, WP, SOI, BEST, EPNP, N34, ONI, EA, TPI, ENSO, N4, PDO, HAW, Q70, EAWR, TNA, PMM, NTA, N1, Q50, AMM, TNI, IND, WHWP, VPM2, RMM2, DMI, VPM1 (RMM1)
Geopot 50 hPa	17 (5)	AAO, AO, NAO, Q50, TNI, PE, N4, N34, TPI, ONI, EPNP (VPM2, PNA, EA, RMM2, RMMN)
Geopot 200 hPa	40 (0)	AAO, AO, NAO, N34, ENSO, N4, TPI, ONI, BEST, SCA, WP, IND, SOI, EPNP, PNA, PE, EA, NOI, WHWP, PDO, EAWR, N1, CAR, VPM1, NTA, Q70, TNA, TNI, HAW, AMO, RMM1, RMM2, PMM, VPM2, EA_ersst, MJ2, FMO2, OOMI2, TSA
Geopot 500 hPa	32 (1)	AAO, NAO, AO, SCA, WP, PNA, PE, EPNP, BEST, EA, EAWR, NOI, ENSO, TPI, N4, SOI, N34, ONI, PDO, HAW, IND, Q70, TNA, PMM, NTA, WHWP, TNI, AMO, N1, Q50 (RMM2)
Geopot 850 hPa	33 (1)	AAO, AO, NAO, PE, SCA, PNA, WP, NOI, BEST, SOI, EPNP, EA, TPI, N4, N34, ENSO, ONI, PDO, EAWR, HAW, Q70, TNA, NTA, PMM, Q50, N1, TNI, IND, WHWP, DMI, VPM2 (RMM1)
Geopot 950 hPa	30 (1)	AAO, AO, NAO, PE, SCA, NOI, PNA, WP, SOI, BEST, EA, ENSO, N34, ONI, TPI, N4, PDO, EPNP, EAWR, HAW, Q70, TNA, NTA, N1, PMM, TNI, IND, Q50 (RMM2)
Zonal winds 200 hPa	51 (0)	BEST, N34, TPI, SOI, ONI, ENSO, N4, IND, PDO, NOI, N1, VPM2, WHWP, RMM2, HAW, AO, NAO, PE, VPM1, AAO, WP, CAR, SCA, EA_ersst, OOMI1, PMM, EPNP, TNI, RMM1, EA, IPO, PNA, NTA, TNA, STA, MJ2, MJ1, TSA, DMI, OOMI2, FMON, AMO, FMO2, AMM, VPMN, RMMN, MJN, FMO1, OOMIN, Q50
Zonal winds 500 hPa	49 (0)	BEST, SOI, ENSO, N34, ONI, NOI, TPI, N4, AO, NAO, PE, WP, EA, PNA, VPM2, RMM2, AAO, SCA, IND, PDO, N1, EPNP, TNA, OOMI1, MJ1, HAW, WHWP, NTA, VPM1, FMO1, EAWR, PMM, TNI, RMM1, MJ2, DMI, EA_ersst, OOMI2, IPO, FMO2, FMON, VPMN, MJN, STA, TSA, Q50, RMMN, CAR, OOMIN
Zonal winds 850 hPa	46 (1)	BEST, AO, ONI, N34, ENSO, SOI, NAO, TPI, N4, PE, WP, NOI, PDO, AAO, N1, PNA, SCA, HAW, IND, EPNP, EA, WHWP, VPM2, VPM1, RMM2, TNI, PMM, EAWR, IPO, TNA, EA_ersst, RMM1, NTA, DMI, MJ1, OOMI1, AMO, FMO1, CAR, STA, Q70, TSA, MJ2, AMM, OOMI2 (FMO2)
Zonal winds 950 hPa	42 (4)	AO, NAO, ONI, BEST, N34, PE, TPI, ENSO, SOI, N4, WP, AAO, PNA, SCA, NOI, PDO, N1, HAW, EA, EPNP, IND, WHWP, EAWR, TNI, PMM, TNA, VPM1, NTA, IPO, VPM2, AMO, EA_ersst, RMM2, DMI, RMM1, Q70, CAR, AMM (OOMI2, MJ1, MJ2, OOMI1)
Meridional winds 50 hPa	24 (3)	AAO, EAWR, EPNP, SCA, EA, PNA, Q50, N34, ONI, BEST, TPI, SOI, IND, ENSO, NOI, N4, Q70, QBO, WP, AO (VPM2, RMM2, PE)
Meridional winds 200 hPa	32 (1)	AAO, N4, BEST, SOI, N34, TPI, ONI, EAWR, ENSO, EPNP, SCA, NAO, NOI, WP, IND, PDO, EA, PNA, RMM2, AO, VPM2, N1, HAW, PMM, WHWP, CAR, TNI, TNA, NTA, Q70 (FMO1)
Meridional winds 500 hPa	34 (0)	AAO, EAWR, SCA, NOI, EPNP, NAO, N4, SOI, BEST, N34, TPI, ONI, ENSO, WP, EA, AO, PNA, TNI, PDO, PMM, VPM2, HAW, RMM2, N1, IND, IPO, PE, TNA, RMM1, NTA, VPM1, CAR, STA

Meridional winds 850 hPa	33 (0)	SCA, AAO, EAWR, NAO, EA, PNA, EPNP, BEST, N34, SOI, TPI, AO, ONI, ENSO, N4, PE, WP, NOI, HAW, PDO, PMM, IND, VPM2, RMM2, N1, TNI, NTA, TNA, WHWP, Q70, IPO, CAR
Meridional winds 950 hPa	32 (0)	SCA, EAWR, AAO, EA, N34, PNA, ONI, NAO, BEST, PE, ENSO, TPI, SOI, N1, AO, N4, EPNP, WP, NOI, PMM, IND, PDO, HAW, TNI, WHWP, DMI, VPM2, RMM2, CAR, AMM, TNA

1945